Dilute measurement-induced cooling into many-body ground states

Josias Langbehn, Kyrylo Snizhko, Igor Gornyi, Giovanna Morigi, Yuval Gefen, Christiane Koch

Dilute Measurement-Induced Cooling into Many-Body Ground States

Josias Langbehn,[1] Kyrylo Snizhko,[2] Igor Gornyi,[3] Giovanna Morigi,[4] Yuval Gefen,[5] and Christiane P. Koch[1,*]

[1] *Dahlem Center for Complex Quantum Systems and Fachbereich Physik, Freie Universität Berlin, Arnimallee 14, Berlin 14195, Germany*

[2] *Université Grenoble Alpes, French Alternative Energies and Atomic Energy Commission (CEA), Grenoble INP, Interdisciplinary Research Institute of Grenoble (IRIG), Quantum Photonics, Electronics and Engineering Laboratory (PHELIQS), Grenoble 38000, France*

[3] *Institute for Quantum Materials and Technologies and Institut für Theorie der Kondensierten Materie, Karlsruhe Institute of Technology, Karlsruhe 76131, Germany*

[4] *Theoretical Physics, Department of Physics, Saarland University, Saarbrücken 66123, Germany*

[5] *Department of Condensed Matter Physics, Weizmann Institute of Science, Rehovot 7610001, Israel*

(Received 21 December 2023; accepted 5 June 2024; published 1 July 2024)

Cooling a quantum system to its ground state is important for the characterization of nontrivial interacting systems and in the context of a variety of quantum information platforms. It can be achieved by employing measurement-based passive steering protocols, where the steering steps are predetermined and are not based on measurement readouts. However, measurements realized by coupling the system to auxiliary quantum degrees of freedom ("detectors") are rather costly and protocols in which the number of detectors scales with system size will have limited practical applicability. Here, we identify conditions under which measurement-based cooling protocols can be taken to the ultimate dilute limit where the number of detectors is independent of system size. For two examples of frustration-free one-dimensional spin chains, we show that steering on a single link is sufficient to cool these systems into their unique ground states. We corroborate our analytical arguments with finite-size numerical simulations and discuss further applications of dilute cooling.

DOI: 10.1103/PRXQuantum.5.030301

I. INTRODUCTION

The ability to control many-body quantum systems is a prerequisite for implementing quantum information processing but also, and more generally, for advances across quantum physics from atomic and molecular all the way to condensed-matter physics. Particular challenges are to identify control strategies that are both scalable with increasing system size and robust to parameter fluctuations. The challenge of robustness can be addressed by so-called quantum reservoir engineering [1], where coupling to a reservoir induces the desired dissipation. In the long-time limit, the system can then be driven into a predesigned target state, irrespective of the initial state. For many-body quantum systems, this allows for preparing pure and possibly highly entangled states or driving the system into nontrivial quantum phases [2–7]. Leveraging the robustness of driven-dissipative dynamics, here we address the challenge of scalability in many-body quantum control. Using control-theoretic arguments, we show under which conditions local cooling into a global target state can be realized.

Our starting point is a recent modification of quantum reservoir engineering where the desired dissipation is induced by quantum measurements [8]. This addresses the problem that, when seeking to exploit engineered dissipation as a resource for, e.g., quantum computation [3,4], the required couplings with the reservoir are difficult or even impossible to design. In other words, natural dissipation processes often do not allow for the system-reservoir interactions needed for, e.g., a given target state, because it involves purely local operators. In quantum measurements, the quantum system of interest is coupled to a "detector" for a time during which the system and detector become entangled (at least weakly), at which point the interaction is switched off [9]. A textbook example is given by a quantized electromagnetic field mode that interacts with

*Contact author: christiane.koch@fu-berlin.de

Rydberg atoms as "detectors" [10]. Depending on the initial state of the atoms, the quantum system can be cooled to zero temperature [10] or prepared in an entangled state [11]. Using the framework of quantum measurements, engineering the required dissipation by coupling to auxiliary degrees of freedom can also be described in terms of so-called quantum collision models [12]. Under both perspectives, the concept of the engineered environment has found a wide range of applications; e.g., for cooling a spin chain by using a qubit as a detector, the frequency of which is tuned to an energy gap of the system [13–15]. Such cooling into low-energy states of the transverse-field Ising model has recently been demonstrated in experiments with superconducting qubits [6]. Engineered dissipation is also central to protocols based on homogenization of quantum systems [16,17] and to "algorithmic" or digital cooling in quantum simulators [18–20].

For a single quantum degree of freedom interacting with one or more detectors, such as the electromagnetic field mode interacting with a beam of atoms [10], any desired state can be prepared with suitably optimized classical drives [21]. As another example, combining measurement-based dynamics with unitary evolution, it is possible to steer a spin-1/2 system to any desired state on or inside the Bloch sphere [22,23]. Such a high level of control is challenging for many-body quantum systems, where the multipartite nature introduces competing time scales and restrictions on the reachable states. For example, only certain classes of states will be attainable with quasilocal couplings [24,25] and systems with frustrated local Hamiltonians are not amenable to passive steering [26]. For many-body quantum systems, measurements can nevertheless be exploited in multiple ways, which include, among many others, inducing phase transitions [27–30], realizing cooling with quantum hardware [14,31–35], protecting quantum states and dynamics [36–38], modifying the entanglement structure [39], or steering a quantum system from an arbitrary initial state toward a chosen target state [22,23,40].

The Affleck-Lieb-Kennedy-Tasaki (AKLT) Hamiltonian [41,42] is a popular many-body model featuring symmetry-protected topological order. It has served as a major paradigm for both quantum reservoir engineering [3] and measurement-induced dynamics, including state engineering [22,43–47] in many-body quantum systems; similar protocols have also been brought forward for the two-dimensional Kitaev model, a spin liquid [48,49]. In this respect, the AKLT model and its relatives could be considered as instrumental tools that bridge the field of measurement-induced state preparation with that of strongly correlated systems.

As much as versatility and robustness make control via coupling to auxiliary degrees of freedom appealing, for many-body quantum systems this comes at a cost. The first distinction is based on whether or not the measurement outcomes are used for control [9]. In the context of steering, this is referred to as passive [22] versus active [40] steering, with passive steering including measurement-induced cooling [14,22,47]. While active steering may leverage decision-making policy [40,50] or optimization [51] to facilitate the approach to the target state, the actual implementation of the feedback requires additional resources, on top of the auxiliary quantum systems serving as detectors [52]. For many-body systems, this will quickly become challenging, if not unfeasible. In fact, already for passive steering protocols, one may wonder how far these can be pushed given their requirement of the number of detectors that is extensive in system size [cf. Fig. 1(a)].

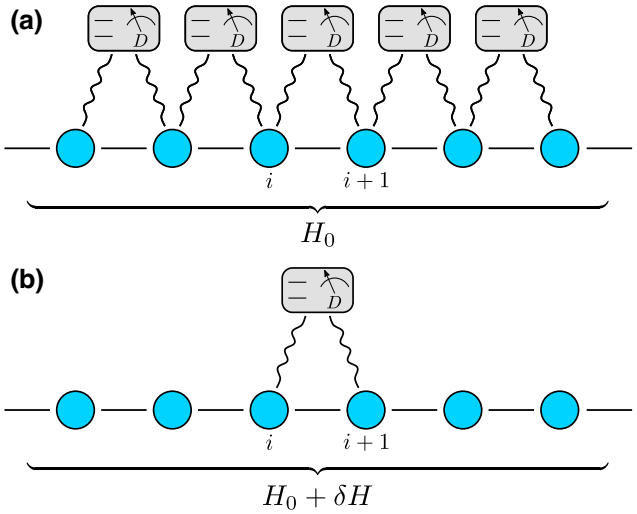

FIG. 1. The measurement-induced cooling of a many-body system described by Hamiltonian H_0 (shown as one-dimensional for simplicity). (a) The setup as discussed in Ref. [22] with an extensive number of detectors D, each one coupled to a pair of sites. (b) Dilute cooling in the extreme limit of a single detector D: the interplay between the local detector-system coupling and possibly additional coherent interactions δH allows for driving the system into the ground state of H_0.

Here, we adopt the perspective that detectors are a precious resource, whereas the ability to engineer (quasilocal) interactions within a many-body system can be taken as given, since this is a prerequisite for implementation of the many-body model itself. The detectors are key to realizing measurement-induced dynamics but how many are actually needed? For the paradigmatic AKLT model, a chain of spin-1 particles, we show that measuring on a single pair of two neighboring sites is sufficient to cool the entire chain into its ground state [cf. Fig. 1(b)]. The reason is that for sufficiently large chains, the nearest-neighbor couplings allow for the propagation of any excitation to the measured link where the excitation is dissipated. While the structure of the AKLT Hamiltonian is such that it ensures the propagation for all conceivable excitations, in general, this is, of course, not the case. We, therefore,

identify which quasilocal Hamiltonians should be added to engineer the necessary population flow and exemplify our theoretical framework for dilute cooling of a many-body system with a second example, the Majumdar-Ghosh model [53]. Finally, we discuss the hierarchy of time scales for the excitation propagation and localized measurements, in order to identify the scaling of the cooling time with the system size, as well as the time dependence of cooling in the limit of infinite systems.

The remainder of the paper is organized as follows. In Sec. II, we present the overall concept of measurement-induced cooling, starting with a brief recap of passive steering [22] and its description in terms of a master equation in Sec. II A. In Sec. II B, we introduce the notions of local hot and cold subspaces on the link(s) that are to be be cooled. This gives rise to conditions on the system-detector couplings to be permissible for a given target state. In other words, the notion of the local hot and cold subspaces allows us to answer the question of when one may perform the measurements that are required to attain the target state. Another key ingredient for many-body cooling is the cooling rate and we explain how to estimate it as a function of the system size in Sec. II C. In Sec. III, we analyze numerically two distinct models defined on finite chains and demonstrate that cooling a single link is sufficient to drive into the respective many-body ground state. For the AKLT model, this is possible for sufficiently large chains, as we discuss in Sec. III A, while we show in Sec. III B, using the Majumdar-Ghosh model, that dilute cooling can also be used to selectively drive into one state within a degenerate ground-state manifold for sufficiently large chains. Dilute cooling is not limited to these two examples and we formulate a general framework in Sec. IV. In Sec. IV A, we formalize the condition to preserve the target for all conceivable interactions within the system. This, together with the corresponding condition on the system-detector couplings, allows us to identify conditions, a necessary one and a sufficient one, for dilute cooling in Secs. IV B and IV C, respectively. With those conditions at hand, we show how to prepare the AKLT state in small chains in Sec. IV D. Readers not interested in the mathematical details of Secs. II B and IV will find a concise summary of the general framework for dilute measurement-induced cooling in the form of a "recipe" in Sec. V. We conclude in Sec. VI.

II. MEASUREMENT-INDUCED COOLING

We first briefly review the protocol of Ref. [22] for steering the state of a quantum system from an arbitrary initial state toward a chosen target state by coupling it to an extensive number of auxiliary quantum degrees of freedom ("detectors") in Sec. II A. Then, we lay the foundations for dilute cooling by introducing the notions of cold and hot subspaces on the cooled sites in Sec. II B. When reducing the number of detectors, a key question is how fast the target state is approached and we discuss in Sec. II C how to estimate the cooling rate (or time) to reach the target state.

A. Recap of passive steering

In the following, we derive an effective Markovian master equation in Lindblad form for the system due to its coupling with the detectors. We do not account for any uncontrolled interactions with the environment, i.e., we assume that the system only interacts with the auxiliary degrees of freedom in a controlled way. For simplicity, the auxiliary quantum degrees of freedom are taken to be qubits. The total Hamiltonian for the composition of system and detector is written as

$$H = H_{\mathrm{s}} \otimes \mathbb{I}_{\mathrm{d}} + H_{\text{s-d}} + \mathbb{I}_{\mathrm{s}} \otimes H_{\mathrm{d}}, \tag{1}$$

where H_{s}, $H_{\text{s-d}}$, and H_{d} act, respectively, on the system only, on the system and detector, and on the detector only, and $\mathbb{I}_{\mathrm{s}}$ ($\mathbb{I}_{\mathrm{d}}$) is the identity operator on the system (detector) Hilbert space. In the following, we drop the explicit reference to the identity operators. The protocol consists of repeatedly performing the following steps [22]:

(1) At time t_i, each detector qubit is prepared in a fixed pure state, independent of the system state. The detector and system are in the product state $\rho_{\mathrm{d}} \otimes \rho_{\mathrm{s}}(t_i)$, where ρ_{d} and ρ_{s} are the state of the detector qubits and that of the system alone, respectively.

(2) System and detector qubits are coupled during a time interval δt. The time evolution generated by the Hamiltonian H is given by

$$\rho_{\text{s-d}}\left(t_i + \delta t\right) = e^{-iH\delta t} \rho_{\mathrm{d}} \otimes \rho_{\mathrm{s}}\left(t_i\right) e^{iH\delta t}, \tag{2}$$

where $\rho_{\text{s-d}}$ denotes the joint state of the system and detector qubits.

(3) At the instant of time $t_{i+1} = t_i + \delta t$, the interaction is switched off and the detector qubits are discarded. This is equivalent to a projective measurement of the detector qubits, with an unbiased average over all measurement outcomes. The system state is then obtained by tracing out the detector qubits:

$$\rho_{\mathrm{s}}\left(t_i + \delta t\right) = \mathrm{Tr}_d \rho_{\text{s-d}}\left(t_i + \delta t\right). \tag{3}$$

The procedure is repeated, starting at time $t_{i+1} = t_i + \delta t$.

The dynamics of the system evolving under this protocol are obtained as follows [22]. For simplicity, we discuss the derivation of the equation of motion for a single detector qubit; the extension to several detectors is straightforward. The choice of the initial state of the detector qubit, $|\phi_0\rangle$, induces a partition on the detector Hilbert space $\mathcal{H}_{\mathrm{d}}$ into two orthogonal subspaces, $\mathcal{H}_{\mathrm{d}} = \mathcal{D}_0 \oplus \mathcal{D}_1$, with $\mathcal{D}_0$ spanned by $|\phi_0\rangle$ and $\mathcal{D}_1 = \mathcal{D}_0^{\perp}$ spanned by $|\phi_1\rangle$

such that $\langle\phi_0|\phi_1\rangle = 0$. Likewise, the composite system-detector Hilbert space $\mathcal{H} = \mathcal{H}_\mathrm{s} \otimes \mathcal{H}_\mathrm{d}$ is partitioned into subspaces

$$\mathcal{H}_i = \mathcal{H}_\mathrm{s} \otimes \mathcal{D}_i \tag{4}$$

for $i = 0, 1$ such that

$$\mathcal{H} = \mathcal{H}_0 \oplus \mathcal{H}_1. \tag{5}$$

We assume $|\phi_0\rangle$ to be an eigenstate of H_d, separated in energy by Δ_ϕ from $|\phi_1\rangle$. The joint Hamiltonian can be represented as

$$H_\text{s-d} = \begin{pmatrix} H_\mathrm{s} + \Delta_\phi \mathbb{I}_\mathrm{s} & \sqrt{\gamma}\tilde{L}^\dagger \\ \sqrt{\gamma}\tilde{L} & H_\mathrm{s} \end{pmatrix}, \tag{6}$$

where γ parametrizes the coupling strength between system and detector and is also referred to as the *dissipation rate*. The non-Hermitian operators $\tilde{L}, \tilde{L}^\dagger$ act on the system whenever the detector state changes from $|\phi_0\rangle$ to $|\phi_1\rangle$ or vice versa. For sufficiently short intervals δt, Eq. (2) can be expanded to second order in δt. Tracing out the detector qubit results in

$$\begin{aligned}\frac{\rho_\mathrm{s}(t+\delta t) - \rho_\mathrm{s}(t)}{\delta t} &= -i\left[H_\mathrm{s}, \rho_\mathrm{s}(t)\right] - \left[H_\mathrm{s}, \left[H_\mathrm{s}, \rho_\mathrm{s}(t)\right]\right]\delta t \\ &\quad + \gamma\,\delta t\left(\tilde{L}\rho_\mathrm{s}(t)\,\tilde{L}^\dagger - \frac{1}{2}\left\{\tilde{L}^\dagger\tilde{L}, \rho_\mathrm{s}(t)\right\}\right).\end{aligned} \tag{7}$$

Taking the limit of continuous measurements ($\delta t \to 0$) while keeping $L = \tilde{L}\sqrt{\delta t}$ constant yields an equation of motion for the reduced state of the system that is of Gorini-Kossakowski-Sudarshan-Lindblad (GKSL) form [54,55]. This exemplifies the formal equivalence between a memoryless interaction with an environment and weak and continuous measurements. The generalization to multiple detector qubits is straightforward and results in a sum over the detector qubits each of which contributes a jump operator L_i,

$$\begin{aligned}\frac{d}{dt}\rho_\mathrm{s}(t) = \mathcal{L}\left(\rho_\mathrm{s}(t)\right) &= -i\left[H_\mathrm{s}, \rho_\mathrm{s}(t)\right] \\ &\quad + \gamma\sum_i\left(L_i\rho_\mathrm{s}(t)\,L_i^\dagger - \frac{1}{2}\left\{L_i^\dagger L_i, \rho_\mathrm{s}(t)\right\}\right),\end{aligned} \tag{8}$$

where $\mathcal{L}$ is the Liouvillian. The idea of passive steering is to choose the operators L_i such that repeated system-detector interactions in the long-time limit drive the system into the target state $\rho_\oplus$, which is often (but not necessarily) the ground state of the system Hamiltonian H_s. This is guaranteed if $\rho_\oplus$ is the unique steady state of $\mathcal{L}$, since then any initial state of the system is driven toward $\rho_\oplus$ [56]. Ideally, the target state is pure, $\rho_\oplus = |\psi_\oplus\rangle\langle\psi_\oplus|$. Passive steering is based on a predefined set of system-detector couplings, which, in contrast to active steering, is not modified in the course of the protocol based on the detector readouts. When the measurement outcomes are completely discarded (even for the termination of steering), such a passive protocol is sometimes also referred to as blind steering. In the context of measurement-based cooling, such protocols can be dubbed "blind cooling"; this term will be utilized throughout the paper.

B. Choice of jump operators

In order to understand how to engineer the system-detector interactions, we determine which jump operators are permissible by asking that they leave the target state $|\psi_\oplus\rangle$ invariant. For simplicity, we will focus on 1D lattices ("chains"), where the geometrical locality of the jump operators is established by involving neighborhoods of two adjacent sites, which we call a *link* $(i, i+1)$. Our considerations are, however, not restricted to 1D systems and the generalization to larger neighborhoods is straightforward. The target state on a given link $(i, i+1)$ is obtained by tracing over all other sites,

$$\rho_\oplus^{(i,i+1)} = \mathrm{Tr}_{\mathcal{H}_i^\complement}\left(\rho_\oplus\right), \tag{9}$$

where $\mathcal{H}_i^\complement \equiv \bigotimes_{j\neq i,i+1}\mathcal{H}_j$ denotes the tensor complement to the local Hilbert space of the link, $\mathcal{H}^{(i,i+1)}$. We seek to cool (empty) all states on a given link $(i, i+1)$ that do not pertain to $\rho_\oplus^{(i,i+1)}$.

As a simple example, consider a qubit with target state $\rho_\oplus = |0\rangle\langle 0|$. Since $|1\rangle$ does not pertain to $\rho_\oplus$, cooling via $L = \sigma^- = |0\rangle\langle 1|$ would be permissible. We can formalize this insight via the support of $\rho_\oplus$. Defining the *support* of a state $\rho_\oplus$ as

$$\mathrm{supp}\,\rho = (\ker\rho)^\perp, \tag{10}$$

the local Hilbert space $\mathcal{H}^{(i,i+1)}$ of the link is partitioned into a hot and a cold local subspace,

$$\mathcal{H}^{(i,i+1)} = \mathcal{V}_\mathrm{cold}^{(i,i+1)} \oplus \mathcal{V}_\mathrm{hot}^{(i,i+1)}, \tag{11a}$$

$$\mathcal{V}_\mathrm{cold}^{(i,i+1)} = \mathrm{supp}\,\rho_\oplus^{(i,i+1)}, \tag{11b}$$

$$\mathcal{V}_\mathrm{hot}^{(i,i+1)} = \left(\mathcal{V}_\mathrm{cold}^{(i,i+1)}\right)^\perp = \ker\rho_\oplus^{(i,i+1)}. \tag{11c}$$

We refer to $\mathcal{V}_\mathrm{hot}^{(i,i+1)}$ as *hot* because it contains all the states that do not pertain to $\rho_\oplus^{(i,i+1)}$ and therefore cooling consists of emptying the hot subspace so that the state of the system is in the *cold* local subspace $\mathcal{V}_\mathrm{cold}^{(i,i+1)}$.

The partitioning of the local Hilbert space of the cooled link into hot and cold subspaces leads to a natural way

of choosing the jump operators: for every state $|\phi_{\mathrm{h},j}\rangle \in \mathcal{V}_{\mathrm{hot}}^{(i,i+1)}$, we choose some state $|\phi_{\mathrm{c},j}\rangle \in \mathcal{V}_{\mathrm{cold}}^{(i,i+1)}$ such that $L_j = |\phi_{\mathrm{c},j}\rangle\langle\phi_{\mathrm{h},j}|$. This choice ensures that the jump operators L_j do nothing but cool, i.e., they do not transfer population from the cold to the hot subspace or within the hot subspace, and they do not result in pure dephasing, but they transfer population into the cold subspace.

This intuition can be formalized in terms of three conditions. First, the operators $L_j^{(i,i+1)}$ must be nilpotent, i.e.,

$$\left(L_j^{(i,i+1)}\right)^2 = 0. \tag{12a}$$

This ensures that all eigenvalues of $L_j^{(i,i+1)}$ are 0. Otherwise, $L_j^{(i,i+1)}$ would possess at least one nonzero eigenvalue, implying the existence of an invariant state. The second property guarantees that only states from the cold subspace are not affected by any of the jump operators:

$$\cap_j \ker L_j^{(i,i+1)} = \mathcal{V}_{\mathrm{cold}}^{(i,i+1)}. \tag{12b}$$

Moreover,

$$\sum_j \mathrm{image}\left(L_j^{(i,i+1)}\right) \subseteq \mathcal{V}_{\mathrm{cold}}^{(i,i+1)}, \tag{12c}$$

since then the jump operators only map states from the hot subspace to the cold subspace but do not act within the hot (respectively, cold) subspace.

C. Cooling rate

Designing the system-detector interaction that drives the system into the desired target state is an important first step. For practical applications of the protocol, the time that is required to attain the target state will be faster than the detrimental effects, which tend to heat up the system. This is also relevant; in particular, for many-body systems. A key question is how this characteristic time scales with the system size.

To quantify the approach to the target state, a suitable figure of merit is needed. A natural choice is the Hilbert-Schmidt overlap,

$$D_{\mathrm{overlap}} = \mathrm{Tr}\left(\rho_{\mathrm{f}}\,\rho_{\oplus}\right), \tag{13}$$

between the obtained state ρ_{f} and the target state $\rho_{\oplus}$. It is a suitable figure of merit as long as the target state is pure [57]. This is the case here and we will use it throughout. For mixed states, one would need to consider a true distance measure [57] such as the Hilbert-Schmidt distance, $D_{\mathrm{HS}} = \frac{1}{2}\mathrm{Tr}\left((\rho_{\oplus} - \rho_{\mathrm{f}})^2\right)$. Since we are interested in cooling, one could also consider the expectation value of the system energy, relative to the targeted energy, i.e., $E_s^{rel} = \mathrm{Tr}\left(H_{\mathrm{s}}\rho_{\mathrm{f}}\right) - \mathrm{Tr}\left(H_{\mathrm{s}}\rho_{\oplus}\right)$.

The rate of cooling is set by the spectral gap of the Liouvillian, defined as $\Delta = |\mathrm{Re}\,\lambda_1|$, where λ_1 is the nonzero eigenvalue of $\mathcal{L}$ with the real part closest to 0. This can be rationalized as follows. Expressing any state ρ in terms of the (right) eigenvectors ρ_i of $\mathcal{L}$, its evolution can be written as $\rho(t) = \sum_i c_i\rho_i e^{\lambda_i t}$, where $c_i = \mathrm{Tr}(\check{\rho}_i\rho)$ is the projection onto the left eigenvector $\check{\rho}_i$. The decay toward the steady state is given by $\mathrm{Re}\,\lambda_i$. The lowest excited state, i.e., the gap, sets the slowest rate of approach toward ρ_0, which dominates in the asymptotic limit $t \to \infty$. The larger the gap, the faster is the convergence toward $\rho_{\oplus}$. If there exist multiple steady states, namely, there are multiple right eigenvectors at eigenvalue 0, then $\Delta = 0$. In this case, for some initial states, the dynamics will not converge to $\rho_{\oplus}$ and blind cooling is not feasible. The uniqueness of the steady state can be checked in terms of the algebraic properties of the Hamiltonian H and the jump operators L_i [58] (see also Ref. [59]).

Obtaining Δ from exact diagonalization quickly becomes unfeasible, since the Liouvillian corresponds to a $d^2 \times d^2$ matrix for a system Hilbert-space dimension d. With the separation of the Hilbert space into cold and hot subspaces introduced above in Sec. II B, and under the assumption of a unique steady state, it is possible to estimate the gap Δ determining the cooling rate for sufficiently small dissipation rates γ as

$$\Delta \lesssim \Delta_{\mathrm{est}}, \tag{14}$$

with the estimate Δ_{est} deriving from the properties of the Hamiltonian:

$$\Delta_{\mathrm{est}} \equiv \frac{1}{2}Q\gamma, \tag{15a}$$

$$Q \equiv \min_{\epsilon} q_{\epsilon}, \tag{15b}$$

$$q_{\epsilon} \equiv \min_{n} \langle\epsilon_n|P_{\mathrm{hot}}|\epsilon_n\rangle. \tag{15c}$$

Here, ϵ labels the (possibly degenerate) eigenenergies of H with the corresponding eigenspace spanned by $|\epsilon_n\rangle$, where n runs over the degenerate eigenstates. The projector P_{hot} projects onto the "hot" subspace on the link $\mathcal{V}_{\mathrm{hot}}^{(1,2)}$ [cf. Eq. (11c)], assuming that this is the only link that is cooled. With these definitions, Q in Eq. (15) gives the minimum population that an excited eigenstate $|\epsilon_n\rangle$ can have in the hot subspace.

The estimate given in Eq. (15) is justified for sufficiently small dissipation rate γ (see Appendix A),

$$\gamma \ll N/d^N, \tag{16}$$

where N is the number of sites, d is the Hilbert-space dimension on a single site, and the Hamiltonian is of the form $H = \sum_i O_i$, with the spectrum of local operators O_i (which can act on site i and neighboring sites) confined

to $[0, 1]$, so that N/d^N is the typical level spacing of the Hamiltonian.

In our numerical studies of the examples below, we find, irrespective of γ, that Δ_{est} provides a bound for the gap,

$$\Delta \leq \Delta_{\text{est}}. \tag{17}$$

We have not been able to prove this bound analytically, yet it looks natural in the light of the following intuition: the cooling rate is determined by the population of the hot subspace (Q) times the dissipation rate (γ), yet may actually be smaller since after local depopulation of the hot subspace, excitations need time to propagate to the cooled link; at the same time, coherent superpositions between the states of different energies evolve in time, as they acquire relative phases—this justifies the focus on the eigenstates of the Hamiltonian.

III. REALIZATION OF SINGLE-LINK COOLING IN TWO FRUSTRATION-FREE SPIN CHAINS

A. Cooling into the AKLT state for $N \geq 5$ sites

The ground state of the AKLT model [41,42] is a paradigmatic example of a matrix product state, as well as of a symmetry-protected topological phase [60]. In the context of quantum engineering, it holds promise as a resource for measurement-based quantum computation [61]. Measurement-assisted preparation of the AKLT ground state has recently attracted much attention [22,40, 44,45,62], as an illustration of proof-of-principle protocols for engineering correlated many-body states. We now show that measurement-induced cooling into the AKLT ground state can be taken to the dilute limit.

The AKLT model [41,42], a 1D chain of spin-1 particles with nearest-neighbor interactions [cf. Fig. 2(a)], is an example of a frustration-free system with a Hamiltonian given by the sum of the noncommuting local Hamiltonians. Periodic boundary conditions (PBCs) imply uniqueness of the ground state, which is a valence-bond state such that on each bond between two neighboring spins, there is no projection on the total spin-2 sector. The ground state of the whole chain is also the ground state of each local term of the "parent Hamiltonian." The latter property is what allows [63] for local steering, i.e., each jump operator needs to act on only one bond. Preparation of the AKLT ground state with passive steering has been shown in Ref. [22] for a total number of detectors that is extensive in system size. In that work, the passive steering protocol has been applied to a system of *noninteracting* spin-1 particles. In the present work, the measurement-induced dynamics are superimposed onto the system dynamics governed by its own interacting Hamiltonian. We show that, remarkably, cooling a single link is sufficient to drive into the AKLT ground state for systems with $N \geq 5$ sites and then we discuss the special case of chain sizes $N = 3, 4$.

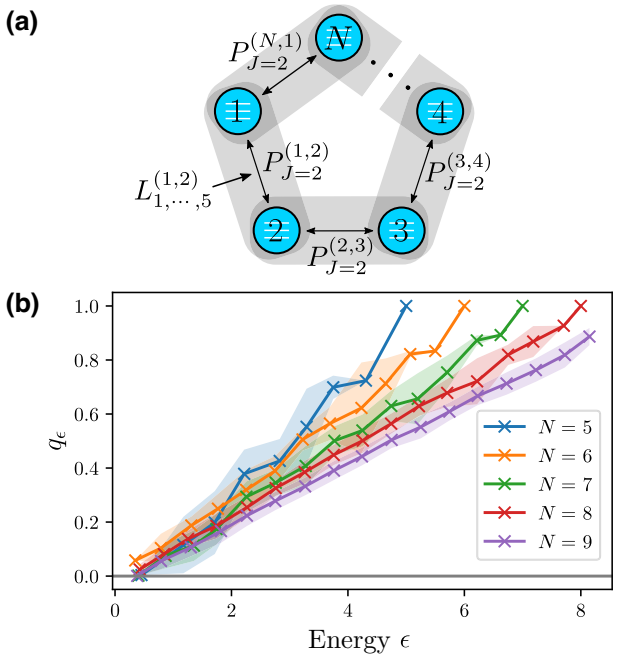

FIG. 2. (a) A schematic of the spin-1 AKLT chain with periodic boundary conditions (PBCs). The projectors onto the $J_i = 2$ subspace for each nearest-neighbor link, $P^{(i,i+1)}_{J=2}$, make up the AKLT Hamiltonian. In its most extreme form, dilute cooling acts on a single link only, via the five cooling operators $L^{(i,i+1)}_{1,\ldots,5}$ [cf. Eq. (19)], with i taken to be $i = 1$. (b) The correlation of the minimal eigenstate projection onto the hot subspace q_ϵ [see Eq. (15b)], with energy ϵ for AKLT chains of increasing size. The solid lines show the mean of q_ϵ for energy bins of size $\Delta E = 0.5$, while the shaded background gives the standard deviation. This correlation implies that, in general, low-lying excitations will decay more slowly than higher-energy ones.

With the nearest-neighbor interaction, two neighboring spin-1 particles can form pairs of total spins $J_i = 0, 1$ or 2, where J_i is the quantum number associated with the eigenvalues of $(\vec{J}_i)^2$, the square of the total spin operator $\vec{J}_i \equiv \vec{S}_i + \vec{S}_{i+1}$. The AKLT Hamiltonian is defined as the sum of the projectors $P^{(i,i+1)}_{J=2}$ on the $J_i = 2$ subspaces, thereby penalizing them energetically:

$$H_{\text{AKLT}} = \sum_{i=1}^{N} P^{(i,i+1)}_2. \tag{18}$$

To drive the system into the ground state of Eq. (18), a possible choice of operators L_i projects each $J_i = 2$ state onto $J_i = 0, 1$ states [22],

$$L^{(i,i+1)}_1 = (|1,1\rangle \langle 2,2|)_{(i,i+1)}\,, \tag{19a}$$

$$L^{(i,i+1)}_2 = (|1,1\rangle \langle 2,1|)_{(i,i+1)}\,, \tag{19b}$$

$$L^{(i,i+1)}_3 = (|1,0\rangle \langle 2,0|)_{(i,i+1)}\,, \tag{19c}$$

$$L_4^{(i,i+1)} = (|1,-1\rangle\langle 2,-1|)_{(i,i+1)}\,, \tag{19d}$$

$$L_5^{(i,i+1)} = (|1,-1\rangle\langle 2,2|)_{(i,i+1)}\,, \tag{19e}$$

where i labels the sites and $|J,m_J\rangle_{(i,i+1)}$ denotes the state of total spin J_i, formed from the spins on the sites $i, i+1$, with projection quantum number m_J. We note that the chosen jump operators are "compatible" with the Hamiltonian of the system in the sense that they do not affect the ground state of the Hamiltonian. Expressions for the jump operators in terms of spin operators can be found in Appendix B.

In Fig. 3, we show how the system state approaches the AKLT ground state as time evolves, for chain lengths up to $N = 10$. Here, the five steering operators are applied to the link connecting sites 1 and 2. The state overlap is calculated by averaging over Monte Carlo trajectories [64] that unravel the GKSL equation given in Eq. (8), resampling 10 000 trajectories 500 times with the bootstrap method [65]. The confidence intervals for the Monte Carlo sampling are smaller than the line widths of the curves. In Fig. 3, we demonstrate an exponential approach to the AKLT ground state for all chain lengths N. The gap Δ is then easily extracted from the slopes in Fig. 3. As one would expect, the approach to the ground state slows down with chain length N, with a clear difference between even and odd numbers of sites, where the ground state is approached faster for even-length chains. This will be further analyzed below, in terms of the gaps.

The overall possibility of dilute cooling and its dependence on system size can be rationalized as follows. Dilute cooling is the result of an interplay between local cooling and coherent nonlocal dynamics generated by the interactions between neighboring sites in the Hamiltonian. While excitations of the chain that are distant from the cooled link are not directly exposed to the jump operators, the interactions propagate them through the chain until they eventually reach the cooled link. Here, cooling takes place, taking energy out of the system by projecting the state onto an energetically lower subspace (from $J = 2$ to $J = 0, 1$). If the state after the jump is the target state, then nothing more happens, since the target state is left invariant by both the jump operators and the interactions. Otherwise, there still exists an excitation somewhere along the chain and the procedure starts over by propagating the excitation through the chain until it reaches the cooled link.

The interplay between dissipation and interaction-induced coherent dynamics naturally introduces two time scales: the dissipative time scale, given by the inverse local cooling rate, $1/\gamma$, is independent of the system size, whereas the time an excitation needs to propagate to the cooled link scales with system size. It is this scaling that explains the slowing down of the approach to the AKLT state observed in Fig. 3.

The slower approach to the AKLT state with increasing system size raises the question as to whether the target state can be attained in the thermodynamic limit. This is determined by the scaling of the Liouvillian gap Δ with the chain length. For our finite-size numerics, in Fig. 4, we have extracted the gaps from the linear fits in Fig. 3 and compared them to the Hamiltonian estimates in Eq. (17). We find a finite gap Δ for chain sizes $N \geq 5$, indicating that cooling a single link drives the system toward $|\mathrm{AKLT}\rangle$ for $t \to \infty$. The gap Δ as a function of system size roughly follows a power law for both even and odd N but with

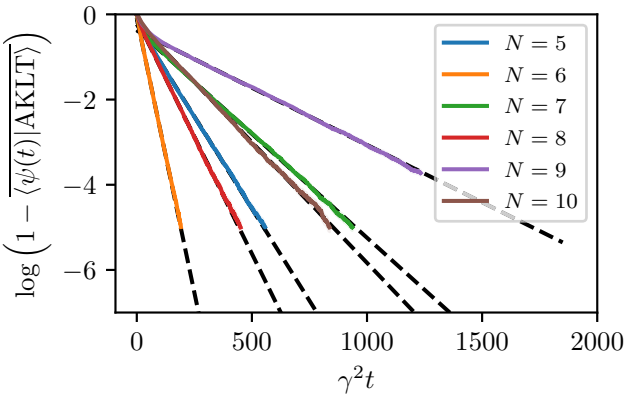

FIG. 3. The logarithm of the overlap with the excited space as a function of time. We observe an exponential approach with time to the AKLT ground state $|\mathrm{AKLT}\rangle$ for weak cooling ($\gamma = 0.1$) on a single link for several chain lengths N. The overlap is obtained from solving Eq. (8) with the Monte Carlo wave-function method (with the bar denoting the average over the Monte Carlo trajectories). The dashed lines are linear fits and their slope is used to extract the Liouvillian gaps.

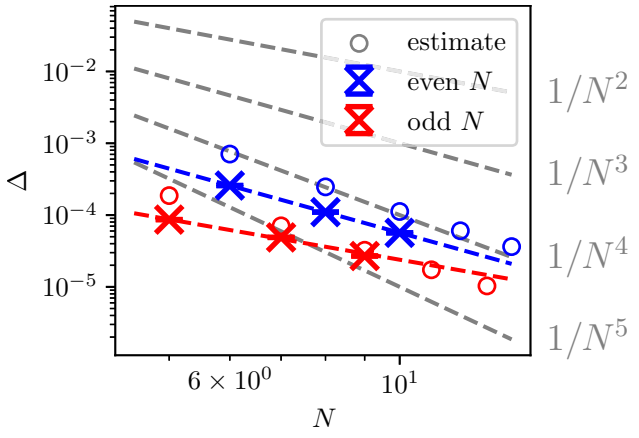

FIG. 4. The Liouvillian gap as a function of the AKLT chain size. The crosses show gaps (with error bars) extracted from the numerical overlaps in Fig. 3, while the circles show gap estimates from Eq. (15). A clear even-odd effect with respect to the chain length is observed, with Δ roughly following a separate power law in the two cases. Fitting to $\Delta(N) = mN^{-\alpha}$ yields exponents $\alpha_{\mathrm{even}} = 2.97$, $\alpha_{\mathrm{odd}} = 1.87$ and y intersects $m_{\mathrm{even}} = 52.3 \times 10^{-2}$ and $m_{\mathrm{odd}} = 17.5 \times 10^{-3}$.

different exponents (cf. Fig. 4). While small chains with even length yield a larger Δ than odd chains of comparable lengths, it is also shown in Fig. 4 that Δ decreases faster with growing even N than it does for odd N.

Chains of size $N = 3, 4$ turn out to be a special case in which single-link cooling fails. This is due to the existence of *dark states*: excited eigenstates that are also stable. These states are not subject to cooling on link 1-2 because on that link they live within the $J_1 = 0, 1$ subspace and thus have no overlap with the local hot subspace. For $N = 3$, there is only a single link with a well-defined spin, as the other spin operators, $\vec{J}_2$ and $\vec{J}_3$, do not commute with $\vec{J}_1$. The *dark states* all show $J_1 = 1$. In a chain with $N = 4$ sites, there can be two links with well-defined spins, e.g., $(1, 2)$ and $(3, 4)$. The *dark states* turn out to feature $J_1 = 0$ and $J_3 = 2$. Starting with $N = 5$, we find no *dark states that are steady states*. With PBCs, $N = 5$ is the smallest chain where any link with the well-defined total spin (meaning that the spin operator of the link in question commutes with J_1) has at least one other link with a well-defined spin between itself and the cooled link. Note that chains of size $N = 3, 4$ can be cooled in a nondilute way, when coupling all links to detector qubits. The failure to cool chains of lengths $N = 3$ and 4 with the steering of a single link can be remedied by adding coherent local interactions. We first identify the general conditions under which dilute cooling is possible in Sec. IV and come back to the AKLT chain with $N = 3, 4$ in Sec. IV D, showing that nearest-neighbor interactions are sufficient.

B. Selective preparation of a degenerate ground state of the Majumdar-Ghosh model

Dilute cooling is, of course, not limited to the AKLT model. We now show that it works equally well for another frustration-free spin chain with a Hamiltonian given as a sum over noncommuting terms, the Majumdar-Ghosh (MG) model [53]. Here, three neighboring spin-1/2 particles are coupled into a total spin with quantum numbers $J_i = 1/2, 3/2$ associated with $\left(\vec{J}_i\right)^2$, where $\vec{J}_i = \vec{S}_i + \vec{S}_{i+1} + \vec{S}_{i+2}$. The original formulation of the MG Hamiltonian was $H_{\mathrm{MG}} = \sum_i^N \vec{J}_i^{\,2}$. Up to a shift in energy, the model can be formulated in terms of projectors such that the $J_i = 3/2$ subspaces are energetically penalized by the projector $P^{(i)}_{J=3/2}$ acting on sites $i, i+1, i+2$ via the Hamiltonian

$$H_{\mathrm{MG}} = 12 \sum_{i=1}^{N} P^{(i)}_{J=3/2}, \tag{20}$$

subject to PBCs. We consider chains with an even number of sites N because the ground-state manifold is only twofold degenerate in this case. It is spanned by the states $|\psi_\pm\rangle$—the product states of spin singlets formed from two neighboring spins with the first spin on an even $(-)$ [respectively, odd $(+)$] site,

$$|\psi_-\rangle = \bigotimes_{i=1}^{N/2} |0,0\rangle_{(2i,2i+1)}\,, \tag{21}$$

$$|\psi_+\rangle = \bigotimes_{i=1}^{N/2} |0,0\rangle_{(2i-1,2i)}\,, \tag{22}$$

where $|0,0\rangle_{(i,i+1)}$ denotes the $S = 0, m = 0$ singlet state on link $(i, i+1)$. Although the ground state is twofold degenerate, it is possible to select one of them with dilute cooling and we choose $|\psi_-\rangle$ as the target ground state.

The ground-state degeneracy represents the main difference between the MG and AKLT models that needs to be accounted for when designing a cooling protocol targeting a pure target state. Naive adaptation of the recipe for choosing the jump operators presented in Sec. II B, considering three neighboring sites of the MG model, suggests projecting every $J = 3/2$ state onto some $J = 1/2$ state. This does not, however, lead to a pure steady state but also allows for statistical mixtures of $|\psi_\pm\rangle$. To single out one of the two ground states $|\psi_\pm\rangle$, it is sufficient to perform cooling on only two neighboring sites. Two neighboring $S = 1/2$ spins combine into either $J = 1$ or $J = 0$. We choose to cool the link $(1, 2)$. The $|\psi_-\rangle$ state lives within the $J = 0$ subspace on this link. A suitable choice of operators that act on the single link $(1, 2)$ transforming the states from the triplet manifold to the singlet manifold is then given by

$$L_1 = (|0,0\rangle\langle 1,1|)_{(1,2)}\,, \tag{23a}$$

$$L_2 = (|0,0\rangle\langle 1,-1|)_{(1,2)}\,, \tag{23b}$$

$$L_3 = (|0,0\rangle\langle 1,0|)_{(1,2)}\,. \tag{23c}$$

For an expression of L_i in terms of spin operators, see Appendix B. This choice implies

$$V^{(1,2)}_{\mathrm{hot}} = \mathrm{span}\left\{(|1,1\rangle)_{(1,2)}\,, (|1,0\rangle)_{(1,2)}\,, (|1,-1\rangle)_{(1,2)}\right\}$$

and $V^{(1,2)}_{\mathrm{cold}} = (|0,0\rangle)_{(1,2)}$. We therefore choose L_i such that any state from $V^{(1,2)}_{\mathrm{hot}}$ is projected into $V^{(1,2)}_{\mathrm{cold}}$. Again in analogy to the AKLT model, excitations outside of the cooled link are propagated through the chain by the interactions, until they eventually reach link $(1, 2)$, where cooling takes place.

The approach to the target state is shown in Fig. 5(a) for chains with an even number of sites up to $N = 16$, where we have used the same numerical method as in Sec. III A. The target state is approached exponentially in time for chains of length $N \geq 6$ with the exponent, i.e., the slope in Fig. 5(a), which depends on N differently for chains with even and odd values of $N/2$. This difference is more clearly seen in Fig. 5(b), where we plot the gap obtained from the

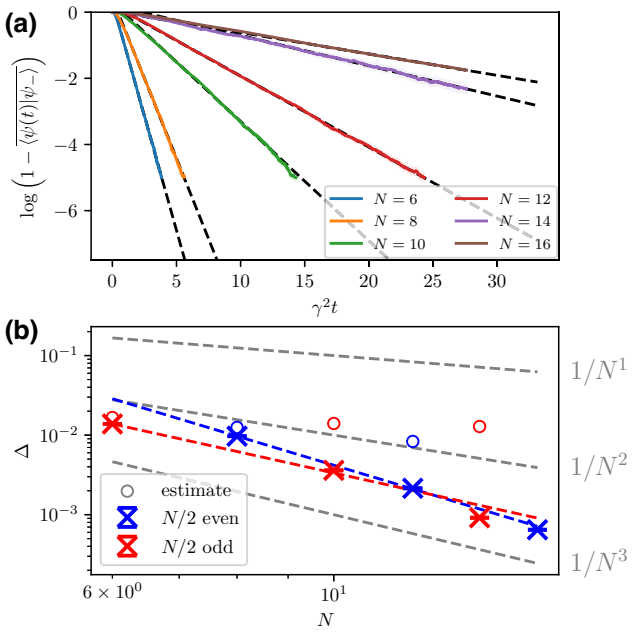

FIG. 5. The scaling of the cooling rate with chain size N for the MG model. (a) The overlap with the target state $|\psi_-\rangle$, bootstrap averaged 500 times over 10 000 trajectories. The dashed lines are linear fits used to extract Δ. (b) The gap fitted to a power law $\Delta(N) = mN^{-\alpha}$. The crosses show gaps (with error bars) extracted from (a), while the circles show gap estimates from Eq. (15), with exponents $\alpha_{N/2\,\mathrm{even}} = 3.76$ and $N_{N/2\,\mathrm{odd}} = 2.78$. The y intersects are $m_{N/2\,\mathrm{even}} = 24.4$ and $m_{N/2\,\mathrm{odd}} = 2.02$.

slopes in Fig. 5(a). The gap estimate in Eq. (15) gives a fairly good prediction of Δ for system size up to $N = 10$ in Fig. 5.

As explained in Appendix A, the estimate can only be expected to give a tight bound if the difference in eigenenergies $\delta\epsilon = |\epsilon - \epsilon'|$ for any pair of energies ϵ, ϵ' is large compared to γ, but for chains with $N \geq 10$, this is no longer the case. The gap roughly follows a power law similar to the AKLT model but the size of the gap is larger by about 2 orders of magnitude compared to the AKLT chains of similar size (cf. Fig. 4). This is in line with the overlaps Q (cf. Eq. (15b)) also being roughly 2 orders of magnitude larger compared to the AKLT model. It is thus easier to scale up the system size in the dilute cooling of the MG model, in the sense that for similar system sizes, the target state will be reached much faster in the MG model as compared to the AKLT state.

IV. CONDITIONS FOR DILUTE COOLING

Detector qubits are a precious resource. In contrast, the ability to engineer quasilocal coherent interactions is a basic prerequisite for the realization of any measurement-induced dynamics—the system needs to be coupled to the detector qubits in the first place. It should then also be comparatively straightforward to alter the Hamiltonian by adding extra terms, as long as they are quasilocal (see also Fig. 1).

This defines a paradigm that allows us to remedy the failure of dilute cooling protocols utilizing only the measurement-induced jump operators, as in the example of the AKLT chain of length $N = 3, 4$. We formulate a general framework to leverage quasilocal interactions to overcome this problem. To this end, we rephrase the key question for dilute cooling: assuming full quasilocal coherent control over the system (in the sense that we are free to add to the system Hamiltonian any quasilocal operator), under which conditions does a desired target state $\rho_\oplus = |\psi_\oplus\rangle\langle\psi_\oplus|$ become the unique steady state of $\mathcal{L}$? In other words, the answer to the question of whether a given $|\psi_\oplus\rangle$ is obtainable via blind dilute cooling does then not depend on H implementing $|\psi_\oplus\rangle$ as its ground state. The necessary condition formalizes the properties that the interaction operators must have in order to leave the target state invariant. The sufficient condition additionally provides a yes-no answer as to whether quasilocal operators with these properties exist that can be added to the Hamiltonian. Readers less interested in the mathematical details may skip the remainder of this section and continue with the discussion of our results in Sec. V.

A. Permissible quasilocal coherent interactions

We restrict ourselves to the case of nearest-neighbor interactions but longer-ranged interactions or more complicated neighborhood definitions are also possible. To set the stage, we first define the space of allowed additional coherent terms. They have to fulfill two conditions: (i) they should be quasilocal and (ii) they need to leave the target state $|\psi_\oplus\rangle$ invariant. A suitable operator basis to represent them is the generalized Pauli basis $\{\sigma_j^i\}$, where $j \leq d^2$, in which d is the dimension of the local Hilbert space on each site i. The space of all quasilocal operators can then be written as

$$\mathcal{O} = \mathrm{span}\ \cup_{i=1}^{N} \mathcal{O}^{(i,i+1)},$$
$$\mathcal{O}^{(i,i+1)} = \mathrm{span}\ \left\{\sigma_j^{(i)} \otimes \sigma_k^{(i+1)} : j, k \leq d^2\right\}.$$

From $\mathcal{O}$, we select those operators that leave $|\psi_\oplus\rangle$ invariant. In the most general sense, this requires $|\psi_\oplus\rangle$ to be an eigenstate to all the selected operators. In order to obtain a vector-space structure, we only allow for selected operators $A \in \mathcal{O}$, such that $|\psi_\oplus\rangle$ is an eigenstate to A with eigenvalue 0. We thus define

$$K_{|\psi_\oplus\rangle} \equiv \{A \in \mathrm{span}\ \mathcal{O} : A|\psi_\oplus\rangle = 0\} \oplus \{\mathbf{1}\}, \tag{24}$$

appropriately dubbing the space of allowed quasilocal coherent terms the *kernelizer*. Note that we do not lose any generality by restricting to annihilators of $|\psi_\oplus\rangle$, since

operators $A \in \mathcal{O}$ with $A|\psi_\oplus\rangle = \lambda|\psi_\oplus\rangle$ and $\lambda \neq 0$ can be obtained by simply adding the identity to $K_{|\psi_\oplus\rangle}$.

The key property of $K_{|\psi_\oplus\rangle}$ as defined in Eq. (24) is to separate the system Hilbert space $\mathcal{H}$ into the target space $\mathcal{H}_\oplus = \text{span}\{|\psi_\oplus\rangle\}$ and its complement $\mathcal{H}_\oplus^\complement$. Our definition in Eq. (24) comes with the advantage that $K_{|\psi_\oplus\rangle}$ has a vector-space structure over $\mathbb{R}$ and contains only Hermitian operators. The kernelizer is thus spanned by all coherent interactions affecting only $H_\oplus^\complement$. The purpose of the separation of Hilbert space is twofold: (i) it allows for identifying the operators that leave the target state invariant and (ii) it implies a straightforward sufficient condition for blind cooling in terms of operator controllability on the complement $H_\oplus^\complement$ (see Sec. IV C).

B. Necessary conditions

We identify two necessary conditions for dilute cooling, one on the jump operators and one on the coherent interactions. The condition on the jump operators formalizes the insight that cooling should not affect the target state, whereas the condition on the coherent interactions is required to ensure population flow to the cooled link. We state the conditions here and prove them in Appendix C.

The condition on the jump operators can be stated as follows. Cooling on a given link $(i, i+1)$ is permissible if the local hot subspace is not empty:

$$\mathcal{V}_{\text{hot}}^{(i,i+1)} \neq \emptyset. \tag{25a}$$

Equivalently, since $\mathcal{H}_{(i,i+1)} = \mathcal{V}_{\text{cold}}^{(i,i+1)} \oplus \mathcal{V}_{\text{hot}}^{(i,i+1)}$, cooling is permissible if the local cold subspace is a proper subset of the local Hilbert space of the link $(i, i+1)$:

$$\mathcal{V}_{\text{cold}}^{(i,i+1)} \subsetneq \mathcal{H}^{(i,i+1)}. \tag{25b}$$

Note that the condition in Eq. (25) is equivalent to Eq. (12): if the hot subspace is not empty, one can always choose a set of jump operators that fulfill Eqs. (12). Conversely, given a set of jump operators obeying the conditions in Eq. (12), a finite hot subspace necessarily has to exist.

Assuming that the condition in Eq. (25) is met, the jump operators $L_j^{(i,i+1)}$ should ideally be chosen as $L_j^{(i,i+1)} = |\phi_{\text{c},j}\rangle\langle\phi_{\text{h},j}|$ such that they map *every* state in $\mathcal{V}_{\text{hot}}^{(i,i+1)}$ to some states in $\mathcal{V}_{\text{cold}}^{(i,i+1)}$, as suggested in Sec. II B. The choice of the $\{L_j^{(i,i+1)}\}$ is not unique. For example, the jump operators for the AKLT chain [see Eq. (19)] map the five states with $J = 2$ onto the four states with $J = 0, 1$ such that the sign of J_z is preserved. Another of many conceivable choices would be $\{L_j^{(i,i+1)}\}$, which flip the sign of J_z.

A necessary condition on the coherent interactions can be stated in terms of the kernelizer. Considering the coherent part of the equation of motion given in Eq. (8), a necessary condition for cooling is that there should be no state other than the target state that is invariant to both cooling and *all* coherent interactions from the kernelizer. In particular, excitations on links that are not cooled have to propagate through the system until they reach the cooled link. We formalize this condition as follows:

$$\nexists\, |\phi\rangle \in \mathcal{H} \setminus \left\{ |\psi_\oplus\rangle \oplus \left(\mathcal{V}_{\text{hot}}^{(i,i+1)} \bigotimes_{j\neq i} \mathcal{H}_j \right) \right\} \text{ such that } |\phi\rangle \text{ is an eigenstate of } \textit{all } A \in K_{|\psi_\oplus\rangle}. \tag{26}$$

The kernelizer contains *all* Hermitian operators that leave the target state invariant, not only those that are part of the system Hamiltonian. This is why the condition in Eq. (26) is necessary but not sufficient.

The condition in Eq. (26) explains why certain states, e.g., the highly entangled Greenberger-Horne-Zeilinger (GHZ) and W states,

$$|\psi_{\text{GHZ}}\rangle = \frac{1}{\sqrt{2}}\left(|0\rangle^{\otimes N} + |1\rangle^{\otimes N}\right), \tag{27}$$

$$|\text{W}\rangle = \frac{1}{\sqrt{N}}\left(|100\ldots0\rangle + |010\ldots0\rangle + \ldots + |00\ldots01\rangle\right), \tag{28}$$

cannot be obtained by dilute cooling. For these states and $N \geq 5$, one can identify a complementary state that is not locally distinguishable from $|\psi_{\text{GHZ}}\rangle$ (respectively, $|\text{W}\rangle$), namely, the antisymmetric GHZ state, $|\phi_{\text{GHZ}}\rangle = \frac{1}{\sqrt{2}}\left(|0\rangle^{\otimes N} - |1\rangle^{\otimes N}\right)$ and the state $|\text{W}_0\rangle = |000\ldots0\rangle$, respectively. Indeed, the reduced states of $|\psi_{\text{GHZ}}\rangle$ and $|\phi_{\text{GHZ}}\rangle$ on any link are identical, which implies that there is no quasilocal operator, neither as part of the Hamiltonian nor as part of the jump operators, that can discriminate between the two states. In contrast, with fewer than five qubits, the condition in Eq. (26) is satisfied and dilute cooling is possible. Given that a link involves two qubits, our argument is in line with the general proof [26] that cooling toward a GHZ state requires measurements on at least $N/2$ qubits [66]. Beyond the framework of Hamiltonians and jump operators with quasilocal interactions that we consider here, dissipative preparation of a GHZ can also be achieved with a single auxiliary degree of freedom, provided that it is coupled globally to all sites [67].

C. Sufficient condition

The understanding that the role of the quasilocal coherent interactions is to ensure population flow toward the cooled link allows us to formulate a sufficient condition for dilute cooling. The desired population flow can surely be realized if *any* unitary evolution on the complement Hilbert space $\mathcal{H}_\oplus^\complement$ is possible. The latter is guaranteed if

the system part that is defined on $\mathcal{H}_{\oplus}^{\mathfrak{C}}$ is controllable and controllability can be checked via the rank of the dynamical Lie algebra [68]. In our case, what matters is the Lie algebra $\mathfrak{L}\left(K_{|\psi_{\oplus}\rangle}\right)$ generated by the kernelizer. The corresponding Lie rank condition reads

$$\dim \mathfrak{L}\left(K_{|\psi_{\oplus}\rangle}\right) = \left(d^N - 1\right)^2 - 1. \tag{29}$$

If Eq. (29) holds, then there exist, in principle, sufficiently many interactions leaving the target state invariant such that any time evolution in $\mathcal{H}_{\oplus}^{\mathfrak{C}}$ can be generated. Since it is a condition purely on the *coherent* part of the dynamics, the necessary condition on the dissipative part in Eq. (25) must also be fulfilled. We note that this condition is sufficient: controllability is a strong assumption and may not be necessary for cooling to work. But if the condition in Eq. (29) is met, then it is possible to add to the Hamiltonian operators from the kernelizer that induce the desired propagation of excitations through the chain toward the cooled link. Thus, Eq. (29) together with Eq. (25) indeed ensures cooling toward $\rho_{\oplus}$.

To illustrate the relationship between population flow and controllability, in Appendix D we verify that the AKLT model in Eq. (18) fulfills the condition in Eq. (29) for unitary controllability in the complement to the target subspace. In fact, it does so for any N. This implies that blind cooling should also be possible for chains of size $N = 3, 4$. In other words, the condition in Eq. (29) tells us how to amend the AKLT Hamiltonian such that blind cooling also becomes possible for the small chains.

D. Use of the sufficient condition to design single-link cooling for the AKLT chain with $N = 3, 4$ sites

For chains of size $N = 3, 4$ and cooling on a single link, multiple steady states exist for the AKLT model. However, since the sufficient condition in Eq. (29) is satisfied for any N (see Appendix D), there exists a coherent interaction δH in the kernelizer, which renders $|\mathrm{AKLT}\rangle$ the unique steady state. One possible choice is to add

$$J_{2,x}^{(i,i+1)} = \sum_{-2 \le m_j \le 2} \left(|2, m_j\rangle\langle 2, m_j + 1|\right)_{(i,i+1)} + h.c. \tag{30a}$$

on all but one link, i.e.,

$$\delta H = \alpha \sum_{i=1}^{N-1} J_{2,x}^{(i,i+1)}. \tag{30b}$$

Since $J_{2,x}^{(i,i+1)}$ only acts on the local $J = 2$ subspace, it is an element of the kernelizer, i.e., permissible. Its specific choice can be motivated as follows. We seek the generator of an evolution that mixes all the excited states to guarantee propagation toward the cooled link. The additional coherent interaction in Eq. (30) mimics the J_x action on the $J = 2$ subspace, generating rotations of the spin around the x axis.

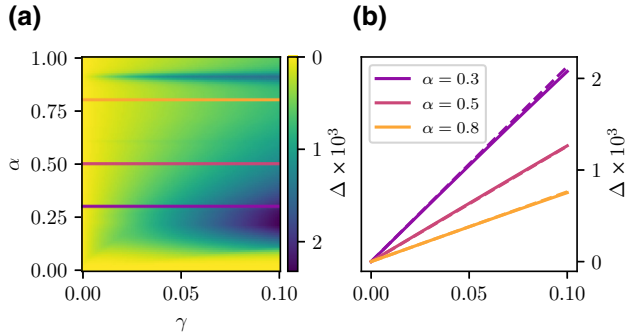

FIG. 6. The Liouvillian gap of the AKLT chain for $N = 3$ with the additional coherent interaction in Eq. (30) on links $(1, 2)$ and $(2, 3)$ as (a) a function of the coherent interaction strength α and the dissipation rate γ and (b) a function of γ for three values of α (solid lines). The gap estimates (cf. Eq. (15)) are also shown (dashed lines). The solid lines in (a) indicate the values of α shown in (b).

Given our choice of δH, whether and how quickly the $|\mathrm{AKLT}\rangle$ is reached will now depend on the interaction strength α and the dissipation rate γ. The rate of approach is determined by the Liouvillian gap, shown in Fig. 6 for $N = 3$ as a function of α and γ. A comparison with the gap estimate in Eq. (15), obtained via exact diagonalization of H_{AKLT}, is also presented in Fig. 6(b). In the weak cooling limit ($\gamma \ll 1$), in which Eq. (8) is valid, the estimate captures the gap very accurately. When the coupling to the detector becomes comparable to or larger than the nearest-neighbor interactions, one would need to solve the full system-detector dynamics [47]. In this regime, the gap is expected to be suppressed due to the quantum Zeno effect, which freezes the coherent evolution. If the dissipation is strong compared to the interactions, the dissipation immediately removes any change to the state due to the interactions, before propagation through the chain can happen. Even in the weak coupling limit, Fig. 6(a) suggests maximizing Δ by proper choice of the relative strengths of the additional coherent interaction and coupling to the detector qubit. More generally, one may also optimize the choice of the additional interactions δH out of all the operators contained in the kernelizer $K_{|\psi_{\oplus}\rangle}$. For $N = 4$, the AKLT model behaves in much the same way, i.e., dilute cooling becomes possible by adding coherent interactions.

More generally, these observations raise the question of how to choose δH. As already mentioned above, this may be viewed as an optimization problem on the kernelizer space, targeting maximum Δ or at least a nonzero gap. Unfortunately, the kernelizer space is high dimensional and the simplest way to approach the question is to randomly sample $\delta H \in K_{|\psi_{\oplus}\rangle}$ and then calculate Δ. We have found in all of 1000 samples that such random sampling

yields δH that results in successful cooling. We are thus led to conjecture that the set of $H \in K_{|\psi_\oplus\rangle}$ not leading to dilute cooling is sparse, possibly of measure zero. This is in line with earlier observations in the context of system size-extensive (i.e., nondilute) steering [26].

V. DISCUSSION: GENERAL FRAMEWORK FOR DILUTE MEASUREMENT-INDUCED COOLING

After showcasing dilute cooling for two paradigmatic many-body models with finite-size numerics, we now turn to the overall applicability of our approach. First, we explore how far one can push the system size in the dilute cooling of many-body systems, given that the approach to the target state slows down as the system size increases. Second, based on a summary of the general framework of dilute cooling, we discuss to which systems it can be applied.

The success of dilute cooling as the size of a many-body system increases depends both on the type and on the strength of the interactions, within the system and of the system with the detector. The interaction strengths give rise to competing time scales, the scaling of which with system size is estimated in the following with the help of a classical diffusion picture. This can readily be motivated by viewing the jump operators as implementing a localized sink for excitations. A classical picture obviously misses many subtleties, e.g., the difference in the propagation speed for classical and nonclassical correlations [69], as well as the possibility of (partial) integrability of the model [70]. Therefore, the scaling arguments presented below will only give a rough estimate for generic correlated systems.

Consider a classical 1D diffusion equation with a δ-function source (or, rather, sink). Denoting the diffusion constant by D and the sink strength by A, the following types of relaxation behavior for a system of size L, characterizing its spatial extent, can be expected (for details of the derivation, see Appendix E):

(1) The "ballistic regime"—for small systems, $L \ll \ell$, where ℓ is the mean free path with respect to the interaction of elementary excitations. The dissipation rate is determined by the measurement rate γ and the many-body level spacing.
(2) The intermediate diffusion regime—for $\ell \ll L \ll D/A$, the decay is exponential with decay time $t_A = L/A$, where $A = \ell\gamma$ and D itself is determined by ℓ (note that the diffusion constant does not enter the decay rate explicitly in this regime).
(3) For large systems, $L \gg D/A$, the time dependence of the survival probability is first given by $t^{-1/2}$, but becomes exponential at $t \gg t_D = L^2/D$, with the "gap" given by $1/t_D$. In the limit of an infinite system, excitations decay in a power-law (more precisely, square-root) manner, implying zero gap for $L = \infty$, as it should be.

For any finite system, all the above regimes correspond to a finite cooling time: for long times, the removal of excitations from the system occurs exponentially. The numerical calculations presented in this work cover the "ballistic regime" of not-too-large systems. Successful cooling in such ballistic systems suggests that the sink satisfies the conditions for cooling in larger systems once diffusion sets in, which guarantees single-sink cooling in an infinite system in the limit of infinite times.

The assumption of quasilocal interactions is key to the competition of time scales as discussed above: for extended systems with quasilocal interactions, the speed with which excitations can propagate to the cooled site(s) is necessarily finite. The picture changes for global interactions, as is the case in, e.g., cavity QED [71], where the upper bound on propagation is set by the system size [72]. Dilute cooling in finite time is then, in principle, possible even in the limit of infinite system size. For large systems with interactions characterized by light-cone propagation of excitations [72], the best strategy for dilute cooling will be to balance "diluteness" with system size. For example, one can conceive a protocol where only every tenth link is cooled, such that the number of "detectors" is still considerably smaller than the number of system sites.

In general, a finite density of detectors will render the cooling time finite in the thermodynamic limit. In practice, our protocol should be used to dilute the number of detectors based on the acceptable cooling times and error levels. Optimization of the performance of the protocol under given constraints will yield the required scaling of the number of detectors with the system size for a given type of interaction. In practice, the optimal protocol performance will be the result of several competing time scales. It will then also be important to account for the finite duration of the measurement [47] when determining how dilute a given protocol can be made, since short system-detector interaction times will need to be compensated by a larger number of detectors.

Next, we provide a simple "recipe" to identify systems amenable to dilute measurement-induced cooling, drawing directly on the examples of the AKLT and MG models:

(1) Consider as target state a ground state of a frustration-free projector-based Hamiltonian.
(2) This state can be stabilized (even without the system's own Hamiltonian) by a frustration-free Lindbladian with local terms acting on all parts of the system.
(3) The local jump operators of such a Lindbladian suggest the form of the local coupling of the system parts (cells) to the measurement apparatus (detector).

(4) In the system with its own Hamiltonian, add the coupling to a detector qubit inferred above only at a single elementary cell of the system (a link, i.e., two neighboring sites in the AKLT and MG examples above).
(5) Unless the Hamiltonian has a perfectly flat band of excitations or there exist excitations that do not overlap with the chosen cell, dilute cooling is expected to work: for a finite system, all excitations will be essentially removed within a finite time.

The simple recipe can be generalized beyond frustration-free projector-based Hamiltonians, such as the AKLT and MG models, and can be made to work even in the case of flat bands or excitations avoiding the sink (as in the $N = 3, 4$ AKLT model). The kernelizer (Sec. IV) is key to this generalization. It allows for identifying Hamiltonians, Lindbladians, and possibly additional interactions to realize dilute cooling. Use of the kernelizer results in the following extension of the simple recipe:

(1) Find a system with a ground state that fulfills the necessary condition in Eq. (25) and choose a set of quasilocal jump operators according to the recipe.
(2) Check if the system fulfills the sufficient condition in Eq. (29) on the kernelizer, i.e., the existence of sufficiently many Hermitian operators acting on the hot subspace only, such that their Lie algebra is of full rank. In other words, check if the system is completely controllable on the (global) hot subspace.
(3) Add as many operators from the kernelizer to the Hamiltonian as needed to ensure a unique steady state.

The most difficult step is the first one but earlier findings for nondilute cooling with quasilocal couplings provide a good starting point [25,26,63]. Good candidates are, e.g., systems with product entangled pair states [3,4,24], including matrix-product states for 1D systems.

VI. CONCLUDING REMARKS

Using quantum measurements or, more generally, coupling to auxiliary quantum degrees of freedom, to engineer desired dissipative dynamics comes with the advantage of versatility and robustness but is also very costly. The scaling of resources for measurement-induced dynamics with system size is an important open but often overlooked question. We have addressed this question for measurement-induced cooling into many-body ground states. Using finite-size numerics and analytical arguments, we have shown that the number of detector qubits can under certain conditions be reduced ("diluted") all the way to the extreme case of a single detector.

In particular, we have demonstrated dilute cooling for two examples: the ground states of the AKLT and MG models. Both are frustration-free spin chains where the Hamiltonian is given by a sum over noncommuting quasilocal terms. In general, cooling or passive steering requires couplings within the system and with the detector that leave the target state invariant. For dilute cooling via weak measurements, this translates into necessary conditions on the jump operators and coherent interactions. To formalize these conditions, we have introduced two key concepts—the kernelizer and the local hot and cold subspaces. The latter are defined via the projection of the target state onto the local Hilbert space of the sites that are cooled. Invariance of the target state is ensured by the jump operators fulfilling Eq. (12) or, equivalently, the local hot subspace not being empty. The kernelizer is the vector space of all quasilocal Hermitian operators that leave the target state invariant. Since these operators generate the flow of excitations toward the cooled site(s), a necessary condition is their mere existence. But the kernelizer is even more useful: it allows us to state a sufficient condition for dilute cooling, in terms of controllability on the Hilbert-space complement to the target state. Controllability of the kernelizer implies the existence of sufficiently many quasilocal Hermitian operators to generate any conceivable unitary evolution on the complementary space. A constructive recipe to implement dilute cooling is then obtained simply by adding coherent interactions from the kernelizer to the Hamiltonian.

One may wonder how robust dilute cooling will be with respect to both undesired decay processes and imperfections in the implementation of the protocol. For a single qubit, quantum steering in the presence of imperfections is found to be fully robust against the erroneous choice of system-detector coupling parameters and reasonably robust against other errors [73]. Unfortunately, these findings cannot simply be transferred to a many-body setting in which the time scales of the cooling, the coherent system dynamics, and the errors, either due to imperfections or undesired decay, all compete. This will be the subject of future work. At the same time, it is important to realize that robustness will not pose a fundamental obstacle to the practical application of dilute measurement-induced cooling. Indeed, the competition of time scales for the desired and undesired dynamics suggests an obvious amendment: if the error rates are too large to admit dilute cooling in the extreme limit of cooling a single link, the diluteness that can be achieved, i.e., the number of detectors relative to the number of system sites, will be determined by the acceptable cooling times and error levels. The recent experimental demonstration of measurement-induced cooling [6] supports this assertion.

Our results are thus relevant for any driven-dissipative dynamics where the desired dissipation is engineered by coupling to auxiliary degrees of freedom. For example, it

is known that the Markovian dynamics of any multipartite open quantum system can be simulated by a multipartite quantum collision model [74]. Our results can be used to improve the scalability and efficacy of multipartite collision models and to determine which states are attainable in open quantum systems with local dissipation. Further, our approach of using controllability to identify couplings within the system that enable dilute cooling is related to the algebraic approach of Ref. [58,75] to determine the operators that ensure uniqueness of the steady state. Combining our conditions for dilute cooling with the algebraic approach of Ref. [58,75] should allow for an even larger class of many-body target states than discussed here. In particular, this will allow for targets beyond ground states.

Future work should also explore dilute steering when treating the system-detector interaction as an adjustable parameter, as has been done in Ref. [47] for nondilute cooling into the AKLT ground state. This is desirable from a twofold perspective: conceptually, it goes beyond the restrictions of the Markovian master equation, allowing us to fully exploit the correspondence with collision models; and in practice, we expect it to yield better more dilute protocols when taking the restrictions of practical detectors into account.

To conclude, we have addressed the challenge of measurement-based cooling a many-body quantum system to its ground state without the costly burden of extensive measurements. By showcasing the effectiveness of cooling on a single link for frustration-free 1D spin chains, we have demonstrated that passive steering protocols can be taken to the dilute limit under specific conditions. Our findings, supported by both analytical arguments and finite-size numerical simulations, emphasize the potential for reducing the resources needed for measurement-induced dynamics. Moving forward, these insights pave the way for further applications, offering a more cost-effective and versatile approach to state engineering and state manipulation in quantum systems.

ACKNOWLEDGMENTS

We thank R. Menu for discussions and gratefully acknowledge financial support from the Deutsche Forschungsgemeinschaft (DFG), Project No. 277101999, from the Collaborative Research Centre (CRC) 183 (project B02), Grants No. EG 96/13-1 and No. GO 1405/6-1, and Project-ID 429529648—TRR306 QuCoLiMa ("Quantum Cooperativity of Light and Matter," project D02), from the German Federal Ministry for Education and Research (BMBF), Project No. 13N16201 NiQ, from the National Science Foundation (NSF)–Binational Science Foundation (BSF) Grant No. DMR-2338819, and from the Israel Science Foundation. This research was supported in part by the NSF under Grants No. PHY-1748958 and No. PHY-2309135. This work is part of the France Hybrid HPC-QC Initiative (HQI) [76] and Application-oriented Benchmarks for Quantum Computing (BACQ) initiatives and is supported by the France 2030 program under the French National Research Agency Grants No. ANR-22-PNCQ-0002 and No. ANR-22-QMET-0002 (MetriQs-France).

Y.G. is the incumbent of an InfoSys Chair.

APPENDIX A: GAP ESTIMATE

Here, we derive the estimate given in Eq. (14) for small dissipation rates γ. We do this by explicitly constructing an eigenstate of the Lindbladian that has eigenvalue $-i\omega-\kappa$ with $\kappa \approx \Delta_{\mathrm{est}}$. Having an eigenstate with $\kappa \approx \Delta_{\mathrm{est}}$ guarantees that the Lindbladian gap does not exceed this value, i.e., $\Delta \lesssim \Delta_{\mathrm{est}}$.

Consider

$$\rho_{\mathrm{coh}} = |\psi_{\mathrm{exc}}\rangle\langle\psi_{\oplus}|, \tag{A1}$$

where $|\psi_{\mathrm{exc}}\rangle \in \mathcal{H}/|\psi_{\oplus}\rangle$ is any state in the excited subspace. ρ_{coh} represents coherences between the target state and the excited subspace and will decay as the population of the excited subspace gets eliminated. Under Eq. (8), the time evolution of the coherences is governed by an effective Hamiltonian,

$$\tilde{H} = H_{\mathrm{s}} - \epsilon_{\oplus} - i\frac{\gamma}{2}P_{\mathrm{hot}}, \tag{A2}$$

where $\epsilon_{\oplus}$ is the ground-state energy of $|\psi_{\oplus}\rangle$ and

$$i\frac{d}{dt}\rho_{\mathrm{coh}} = \tilde{H}\rho_{\mathrm{coh}},$$

where we have used the identities $\langle\psi_{\oplus}|L_i^{\dagger} = 0$ and $\sum_i L_i^{\dagger}L_i = P_{\mathrm{hot}}$. Therefore, any eigenstate $|\lambda\rangle$ of the non-Hermitian Hamiltonian $\tilde{H}$ restricted to the excited subspace gives rise to an eigenstate of the Lindbladian governing the evolution in Eq. (8):

$$\tilde{H}|\lambda\rangle = \lambda|\lambda\rangle \Rightarrow \mathcal{L}(|\lambda\rangle\langle\psi_{\oplus}|) = -i\lambda|\lambda\rangle\langle\psi_{\oplus}|. \tag{A3}$$

For $\gamma \to 0$, the eigenstates of $\tilde{H}$ coincide with the eigenstates $|\epsilon\rangle$ of H_{s} up to corrections $O(\gamma/\delta\epsilon)$, where $\delta\epsilon$ represents the level spacing of H_{s}. Then, by virtue of first-order perturbation theory, the respective decay eigenvalues are $\kappa = -\mathrm{Re}(-i\lambda) = -\mathrm{Im}\,\lambda = (\gamma/2)\langle\epsilon|P_{\mathrm{hot}}|\epsilon\rangle$ up to corrections $O(\gamma^2/\delta\epsilon)$. In the case of degenerate eigenstates of H_{s}, one needs to diagonalize P_{hot} in each energy subspace in order to find the eigenstates of $\tilde{H}$. The smallest $\kappa = \Delta_{\mathrm{est}}$ corresponds to the state $|\epsilon\rangle$ with the smallest overlap with the hot subspace, leading to Eq. (15b).

APPENDIX B: PHYSICAL REPRESENTATION OF JUMP OPERATORS

We present the jump operators introduced above in terms of spin operators to provide a more physical picture of the required interaction. Since the system-detector Hamiltonian $H_{\text{s-d}}$ in Eq. (1) acts on a link, i.e., two system sites, it involves a three-body interaction. It can always be written as $H_{\text{s-d}} = \sigma^\dagger L + \sigma L^\dagger$ where σ (respectively, $\sigma^\dagger$) effects transitions between $|\phi_0\rangle$ and $|\phi_1\rangle$ on the detector.

For the AKLT model, we find that

$$
\begin{aligned}
L_1 &= \frac{1}{8}S_z \otimes S_- + \frac{1}{4}S_z \otimes S_{z,-} + \frac{1}{8}S_z^2 \otimes S_- + \frac{1}{4}S_z^2 \otimes S_{z,-} - \frac{1}{8}S_- \otimes S_z - \frac{1}{8}S_- \otimes S_z^2 - \frac{1}{4}S_{z,-} \otimes S_z - \frac{1}{4}S_{z,-} \otimes S_z^2,\\
L_2 &= -\frac{1}{8}S_z \otimes S_z^2 + \frac{1}{8}S_z \otimes S_{+,-} + \frac{1}{8}S_z^2 \otimes S_z + \frac{1}{8}S_z^2 \otimes S_{+,-} - \frac{1}{8}S_{+,-} \otimes S_z - \frac{1}{8}S_{+,-} \otimes S_z^2 + \frac{1}{16}S_+ \otimes S_- + \frac{1}{8}S_+ \otimes S_{z,-}\\
&\quad - \frac{1}{16}S_- \otimes S_+ - \frac{1}{8}S_- \otimes S_{z,+} + \frac{1}{8}S_{z,+} \otimes S_- + \frac{1}{4}S_{z,+} \otimes S_{z,-} - \frac{1}{8}S_{z,-} \otimes S_+ - \frac{1}{4}S_{z,-} \otimes S_{z,+},\\
L_3 &= \frac{\sqrt{3}}{12}S_z \otimes S_z^2 - \frac{\sqrt{3}}{12}S_z^2 \otimes S_z + \frac{\sqrt{3}}{24}S_+ \otimes S_- - \frac{\sqrt{3}}{12}S_+ \otimes S_{z,-} + \frac{\sqrt{3}}{24}S_+^2 \otimes S_-^2 - \frac{\sqrt{3}}{24}S_- \otimes S_+ - \frac{\sqrt{3}}{12}S_- \otimes S_{z,+}\\
&\quad - \frac{\sqrt{3}}{24}S_-^2 \otimes S_+^2 + \frac{\sqrt{3}}{12}S_{z,+} \otimes S_- - \frac{\sqrt{3}}{6}S_{z,+} \otimes S_{z,-} + \frac{\sqrt{3}}{12}S_{z,-} \otimes S_+ + \frac{\sqrt{3}}{6}S_{z,-} \otimes S_{z,+},\\
L_4 &= -\frac{1}{8}S_z \otimes S_z^2 + \frac{1}{8}S_z \otimes S_{+,-} + \frac{1}{8}S_z^2 \otimes S_z - \frac{1}{8}S_z^2 \otimes S_{+,-} - \frac{1}{8}S_{+,-} \otimes S_z + \frac{1}{8}S_{+,-} \otimes S_z^2 + \frac{1}{16}S_+ \otimes S_-\\
&\quad - \frac{1}{8}S_+ \otimes S_{z,-} - \frac{1}{16}S_- \otimes S_+ + \frac{1}{8}S_- \otimes S_{z,+} - \frac{1}{4}S_{z,+} \otimes S_- + \frac{1}{4}S_{z,+} \otimes S_{z,-} + \frac{1}{8}S_{z,-} \otimes S_+ - \frac{1}{4}S_{z,-} \otimes S_{z,+},\\
L_5 &= \frac{1}{8}S_z \otimes S_+ - \frac{1}{4}S_z \otimes S_{z,+} - \frac{1}{8}S_z^2 \otimes S_+ + \frac{1}{4}S_z^2 \otimes S_{z,+} - \frac{1}{8}S_+ \otimes S_z + \frac{1}{8}S_+ \otimes S_z^2 + \frac{1}{4}S_{z,+} \otimes S_z - \frac{1}{4}S_{z,+} \otimes S_z^2,
\end{aligned}
$$

where $S_{x,y,z}$ are the usual spin operators, $S_\pm = S_x \pm iS_y$, and $S_{a,b} = (S_aS_b + S_aS_b)/2$ with $a, b \in \{x, z, y, +, -\}$ denotes the symmetrized mean.

For the Majumdar-Ghosh model, the jump operators can be rewritten as

$$L_1 = \frac{1}{\sqrt{8}}(\mathbf{1} \otimes S_- - S_- \otimes \mathbf{1}) + \frac{1}{\sqrt{2}}(S_z \otimes S_- - S_- \otimes S_z), \tag{B1}$$

$$L_2 = \frac{1}{2}(S_z \otimes \mathbf{1} - \mathbf{1} \otimes S_z + S_+ \otimes S_- - S_- \otimes S_+), \tag{B2}$$

$$L_3 = \frac{1}{\sqrt{8}}(S_+ \otimes \mathbf{1} - \mathbf{1} \otimes S_+) + \frac{1}{\sqrt{2}}(S_+ \otimes S_z - S_z \otimes S_+). \tag{B3}$$

It should be noted that while the above expressions appear rather lengthy, the jump operators that we consider are just one specific choice. Different choices that are simpler and easier to implement experimentally may exist.

APPENDIX C: PROOFS OF THE NECESSARY CONDITIONS FOR DILUTE COOLING

Here, we provide proofs of the necessary and sufficient conditions for dilute cooling stated in Sec. IV B.

A jump operator is permissible if it leaves the target state invariant in the sense that $L^{(i,i+1)} \otimes \mathbb{1}^{\mathbb{C}} |\psi_\oplus\rangle = 0$. Not all operators with this property lead to cooling, which is why this is only a necessary condition. As a first step, we prove that a necessary condition for the existence of a nontrivial (i.e., nonzero) permissible jump operator on link $(i, i+1)$ is for the reduced density operator to not be full rank. This can be seen to be equivalent to the condition of a nonempty local hot subspace [see Eq. (25a)] by recalling the definition in Eq. (11c) and using that any linear operator has full rank if and only if its kernel contains only 0.

For convenience of notation, we write $L = L^{(i,i+1)}$, assuming that the jump operator only acts on the cooled link $(i, i+1)$.

Claim. $L \otimes \mathbb{1}^{\mathbb{C}} |\psi_\oplus\rangle = 0 \Rightarrow \operatorname{rk} \rho_\oplus^{(i,i+1)} < d^2$.

We prove the contraposition

$$\operatorname{rk} \rho_\oplus^{(i,i+1)} = d^2 \Rightarrow L \otimes \mathbb{1}^{\mathbb{C}} |\psi_\oplus\rangle \neq 0.$$

Consider the right-hand side; it is equivalent to

$$L \otimes \mathbb{1}^{\mathbb{C}} |\psi_\oplus\rangle \langle\psi_\oplus| L^\dagger \otimes \mathbb{1}^{\mathbb{C}} \neq 0. \tag{C1}$$

Since the left-hand side of Eq. (C1) is a projector and using the cyclicity of the trace,

$$\mathrm{Tr}\left(L^\dagger L \otimes \mathbb{1}^{\complement} \left|\psi_\oplus\right\rangle \left\langle\psi_\oplus\right|\right) \neq 0.$$

Taking the partial trace over all but the cooled link allows us to rewrite Eq. (C1) in terms of the reduced state,

$$\mathrm{Tr}\left(L\rho_\oplus^{(i,i+1)}L^\dagger\right) \neq 0.$$

By assumption, $\rho_\oplus^{(i,i+1)}$ has full rank and we may write

$$\rho_\oplus^{(i,i+1)} = \sum_{n=1}^{d^2} \lambda_n \left|n\right\rangle \left\langle n\right|,$$

with $\lambda_n > 0$ and $\{|n\rangle\}$ an orthonormal basis of $\mathcal{H}_{i,i+1}$. Then, the above trace becomes $\sum_n \lambda_n \mathrm{Tr}\left|\tilde{n}\right\rangle\left\langle\tilde{n}\right|$, with $\left|\tilde{n}\right\rangle \equiv L\left|n\right\rangle$. Therefore, $\sum_n \lambda_n \mathrm{Tr}\left|\tilde{n}\right\rangle\left\langle\tilde{n}\right| > 0$ unless $\left|\tilde{n}\right\rangle = 0$ for all n. Since L is required to be nontrivial, we can exclude this case, which concludes the proof.

We now turn to the necessary condition on the coherent interactions, given in Eq. (26). To grasp the intuition, consider a state $|\phi\rangle$ that is neither the target state nor in the hot subspace. Because it is not in the hot subspace, it cannot be affected by any jump operator (we have introduced the jump operators to only act on the hot subspace). Then, $|\phi\rangle$ is not directly subject to cooling, and cooling can only be mediated through interactions. In order for this to work, there has to be some interaction H from the kernelizer that connects $|\phi\rangle$ to some other state $\left|\phi'\right\rangle = H\left|\phi\right\rangle$. It may be that $\left|\phi'\right\rangle$ is then subject to cooling or that $\left|\phi'\right\rangle$ is connected via interactions to yet another state until eventually a state subject to cooling is reached. This observation can be phrased as a necessary condition on the interactions: for every such state $|\phi\rangle$ that is not directly subject to cooling, there has to exist an operator from the kernelizer that maps $|\phi\rangle$ to some other state $\left|\phi'\right\rangle \neq \lambda\left|\phi\right\rangle$ for some $\lambda \in \mathbb{C}$. We formalize this condition as

$$\forall \left|\phi\right\rangle \in \mathcal{H} \setminus \left\{\left|\psi_\oplus\right\rangle \oplus \left(\mathcal{V}_{\mathrm{hot}}^{(i,i+1)} \bigotimes_{j\neq i} \mathcal{H}_j\right)\right\}$$
$$\exists H \in K_{|\psi_\oplus\rangle} : \left|\phi'\right\rangle = H\left|\phi\right\rangle \neq \lambda\left|\phi\right\rangle.$$

Negating both parts of the statement leads to Eq. (26): there can be no state $|\phi\rangle$ being neither the target nor in the hot subspace such that $|\phi\rangle$ would be an eigenstate to all operators from the kernelizer.

APPENDIX D: UNITARY CONTROLLABILITY FOR THE AKLT MODEL

As an illustrative example, here we show that the sufficient condition for dilute cooling on the interactions, Eq. (29), i.e., full unitary controllability on the complement of the target state, is satisfied for the AKLT chain. Our argument consists of three steps. First, we present the general structure of a subset of the kernelizer for the AKLT model. Although only a subset of the kernelizer, we show in the third step that it generates an algebra of full rank on the complement space. Therefore control on this subset leads to full operator controllability on the complement space. Second, we argue that the absence of nontrivial invariant subspaces of the Lie algebra generated by the kernelizer implies controllability. Finally, we present the proof that there can be no other invariant subspaces of the Lie algebra than the space complementary to the target state and the target state itself.

First note that by construction, $|\psi_{\mathrm{AKLT}}\rangle$ is orthogonal to the $J_i = 2$ sectors. Its reduced state on the cooled link, $\rho_{\mathrm{AKLT}}^{(i,i+1)}$, only has support in the $J_i = 0, 1$ subspaces and may in general have $3+1$ nonzero eigenvalues. Moreover, H_{AKLT} makes no distinction between all $J_i = 1$ states such that the eigenvalues of $\rho_{\mathrm{AKLT}}^{(i,i+1)}$ are $(3+1)$-fold degenerate. Labeling them $\lambda_1 = \lambda_2 = \lambda_3 \equiv \lambda$ and λ_0, we may write

$$\rho_{\mathrm{AKLT}}^{(i,i+1)} = \mathrm{diag}\left(\underbrace{0,0,0,0,0}_{J_i=2}, \underbrace{\lambda,\lambda,\lambda}_{J_i=1}, \underbrace{1-3\lambda}_{J_i=0}\right).$$

Evidently, any action on the $J_i = 2$ subspace leaves $\rho_{\mathrm{AKLT}}^{(i,i+1)}$ invariant. Therefore, the local kernelizer, $K_{|\psi_{\mathrm{AKLT}}\rangle}^{(i,i+1)} \equiv K_{|\psi_{\mathrm{AKLT}}\rangle} \cap \mathcal{O}^{(i,i+1)}$, where $\mathcal{O}^{(i,i+1)}$ is the space of operators on the link $(i, i+1)$ (cf. Sec. IV A) is 25-fold dimensional, containing all the generators of unitaries acting on the $J_i = 2$ subspace. In other words, $K_{|\psi_{\mathrm{AKLT}}\rangle}^{(i,i+1)} = \mathfrak{su}(5)$, the generator of $SU(5)$ acting on the $J_i = 2$ subspace.

Since $\mathcal{O}$ is the space of all quasilocal interactions, we may express the (global) kernelizer as

$$\begin{aligned} K_{|\psi_{\mathrm{AKLT}}\rangle} &= K_{|\psi_{\mathrm{AKLT}}\rangle} \cap \mathcal{O} \\ &= K_{|\psi_{\mathrm{AKLT}}\rangle} \cap \left(\mathcal{O}^{(1,2)} + \mathcal{O}^{(2,3)} + \ldots + \mathcal{O}^{(N,N+1)}\right). \end{aligned}$$

This implies that

$$K_{|\psi_{\mathrm{AKLT}}\rangle} \cap \mathcal{O}^{(i,i+1)} \subseteq K_{|\psi_{\mathrm{AKLT}}\rangle}$$

and we have

$$\sum_{i=1}^{N} K_{|\psi_{\mathrm{AKLT}}\rangle}^{(i,i+1)} \subseteq K_{|\psi_{\mathrm{AKLT}}\rangle}.$$

We proceed by showing that the Lie algebra generated by the sum of the local kernelizers is already sufficient to satisfy Eq. (29). For brevity, we write $\mathfrak{L}\left(K_{|\psi_\oplus\rangle}\right) = \mathfrak{L}$ and $K_{|\psi_\oplus\rangle} = K$ in the remainder of the proof and argue that if the Lie algebra $\mathfrak{L}$ acting on a vector space V only

possesses a single invariant subspace, this subspace is V itself. Moreover, in this case the dimension of $\mathfrak{L}$ is maximal, $\dim \mathfrak{L} = \dim V^2$. If it was smaller, then $\mathfrak{L}$ would not generate all unitaries on V and there would be a subspace invariant under $\mathfrak{L}$. It is thus sufficient to prove that $\mathfrak{L}$ possesses exactly two invariant subspaces, $V \oplus |\psi_{\mathrm{AKLT}}\rangle = \mathcal{H}$. The invariance of the latter subspace follows by construction. In other words, it is sufficient to show that there exists no invariant subspace V with dimension smaller than $\dim V = d^N - 1$.

The strategy of the proof is to construct V via repeated applications of $\mathfrak{L}$ on some initial state, chosen to be the all-up state $|v_0\rangle \equiv |1, \ldots, 1\rangle$ in the local spin-1 basis. For lack of an explicit expression for $\mathfrak{L}$, we will only consider actions of $K \subset \mathfrak{L}$ for the generation of V. We shall see that this is already sufficient. We introduce the notation for vector-space orbits, $K[\mathcal{H}] = \mathrm{span}\ \{A|\psi\rangle : A \in K, |\psi\rangle \in \mathcal{H}\}$; it is the image of Hilbert space $\mathcal{H}$ (i.e., a vector space of states) under the vector space of operators K. As a first step, we prove the following.

Lemma 1. There exists some $k \in \mathbb{N}$ such that $V \equiv V^k \equiv \mathfrak{L}[|v_0\rangle]$ is the smallest subspace invariant under $\mathfrak{L}$ and contains $|v_0\rangle$.

Proof. First, by definition, $\mathbf{1} \in \mathfrak{L}$ such that $|v_0\rangle \in V$. For the same reason, we have $V^k \subseteq V^{k+1}$. Therefore, there exists some $k \in \mathbb{N}$ for which the series converges and $V^{k+1} = V^k \equiv V$. Next, we show that indeed there is no smaller subspace that is invariant under $\mathfrak{L}$ and contains $|v_0\rangle$. By definition of V^k, there exists a series of $A_1, \ldots, A_k \in \mathfrak{L}$ such that any $|v\rangle \in V^k$ is connected to $|v_0\rangle$ via $A_k \ldots A_1 |v_0\rangle = |v_1\rangle$. Therefore, V does not contain any subspace that would be invariant under $\mathfrak{L}$. Now assume the existence of smaller subspace W that is invariant under $\mathfrak{L}$ and that contains $|v_0\rangle$. Since we are looking for the smallest such subspace, W cannot contain another subspace that is invariant under $\mathfrak{L}$. This implies that all $|w\rangle \in W$ are connected to $|v_0\rangle$ by some $A_q \ldots A_1 |w\rangle = |v_0\rangle$. By assumption, V^k is converged, so that any such state $|w\rangle$ is also in V. Therefore, $W \subseteq V$ and because neither contains additional invariant subspaces, we have $W = V$. ■

To set the stage for constructing V, we introduce the shorthand notation $K = \sum_{i=1}^{N} K^i$, with $K^i \equiv K^{(i,i+1)}_{|\psi_{\mathrm{AKLT}}\rangle}$, and note that the local Hilbert space on a single link $(i, i+1)$ is partitioned into a local excited space and a local ground space,

$$\mathcal{H}^i = \mathcal{H}^i_2 \oplus \mathcal{H}^i_{0,1},$$

where $\mathcal{H}^i_{2/(1,0)} \equiv \mathcal{H}^{(i,i+1)}_{2/(0,1)}$ refers to the $J = 2$ (respectively, $J = 0, 1$) subspace. The state $|v_0\rangle$ is excited with respect to this partition on all links of the chain and can be expressed locally as $|J = 2, m_j = 2\rangle$ on any link. To carry out the proof, we will first show controllability for even chain lengths and then use the result to prove controllability for odd chain lengths.

For even chain lengths, we can cover the whole chain by the set of adjacent nonoverlapping even (odd) links, denoting a link as even (odd) when the index of the left site is even. In the following, we focus on a cover of the chain by the set of odd links $(1,2), (3,4), \ldots, (N-1, N)$. The spin operators J_i for even and odd i are then mutually commuting, such that any state can be labeled by its J, m_j quantum numbers, and we can partition the total Hilbert space,

$$\begin{aligned}
\mathcal{H} &= \bigotimes_{i=1,\ \mathrm{odd}}^{N} \left(\mathcal{H}^i_2 \oplus \mathcal{H}^i_{0,1}\right) \\
&= \sum_{k=0}^{N} \binom{N}{k} \underbrace{\mathcal{H}_2 \otimes \ldots \otimes \mathcal{H}_2}_{N-k} \otimes \underbrace{\mathcal{H}_{0,1} \otimes \ldots \otimes \mathcal{H}_{0,1}}_{k} \\
&= \sum_{k=0}^{N} \sum_{(p,q) \in P^N_k} \underbrace{\mathcal{H}_2^{p(1)} \otimes \ldots \otimes \mathcal{H}_2^{p(N-k)}}_{N-k} \\
&\qquad \otimes \underbrace{\mathcal{H}_{0,1}^{q(1)} \otimes \ldots \otimes \mathcal{H}_{0,1}^{q(k)}}_{k},
\end{aligned}$$

where P^N_k denotes the set of permutations of an N-dimensional vector of k entries equal to 0 and $N-k$ entries equal to 1. Here q (respectively, p) in $(p,q) \in P^N_k$ denote the positions of the entries 1, (respectively, 0) in the permutation. We illustrate this for the example of an $N = 4$ chain:

$$\begin{aligned}
\mathcal{H} &= \left(\mathcal{H}^1_2 \oplus \mathcal{H}^1_{0,1}\right) \otimes \left(\mathcal{H}^2_2 \oplus \mathcal{H}^2_{0,1}\right) \\
&= \left(\mathcal{H}^1_2 \otimes \mathcal{H}^2_2\right) \oplus \left(\mathcal{H}^1_2 \otimes \mathcal{H}^2_{0,1}\right) \oplus \left(\mathcal{H}^1_{0,1} \otimes \mathcal{H}^2_2\right) \\
&\quad \oplus \left(\mathcal{H}^1_{0,1} \otimes \mathcal{H}^2_{0,1}\right).
\end{aligned}$$

We will show that each such Hilbert-space summand except $\mathcal{H}^1_0 \otimes \ldots \otimes \mathcal{H}^{N-1}_0$ is connected to $|v_0\rangle$ by repeated actions K.

As a first step, consider the action of K^i on $|v_0\rangle$. Note that $|v_0\rangle \in \mathcal{H}^{\mathrm{odd}}_2 \equiv \bigotimes_{i=1,\ \mathrm{odd}}^{N} \mathcal{H}^i_2$ and K^i contains any (Hermitian) operator on $\mathcal{H}^i_2$. Therefore, the vector-space orbit $K^i|v_0\rangle = \mathrm{span}\left\{A|v_0\rangle : A \in K^i\right\}$ contains any state of the form $|2, m_j\rangle_i \bigotimes_{j=1 j\neq i,j\ \mathrm{odd}}^{N} |2,2\rangle$ with $-2 \le m_j \le 2$, i.e., the whole $\mathcal{H}^i_2$. Since for every i the vector-space orbit $K^i|v_0\rangle$ is connected to $|v_0\rangle$ by K, it follows that they all belong to V such that $\mathcal{H}^{\mathrm{odd}}_2 \subset V$.

Next, we show that we can generate a Hilbert-space summand $\mathcal{H}^i_{0,1}$ at an arbitrary position i from $\mathcal{H}^{\mathrm{odd}}_2$. We consider the local kernelizer K^{i+1} acting on the *even* link on $i+1$. Specifically, we consider the image of $\mathcal{H}^{\mathrm{odd}}_2$ under K^{i+1}. Since links i and $i+1$ (respectively, i and

$i-1$) are overlapping, the action of K^{i+1} is nontrivial only on $\mathcal{H}_2^i \otimes \mathcal{H}_2^{i+2}$ and it is sufficient to consider the vector-space orbit $K^{i+1}\left[\mathcal{H}_2^i \otimes \mathcal{H}_2^{i+2}\right]$. One can show (numerically) that it has a finite overlap with $\mathcal{H}_2^i \otimes \mathcal{H}_0^{i+2}$ and $\mathcal{H}_0^i \otimes \mathcal{H}_2^{i+2}$. More specifically, $K^{i+1}\left[\mathcal{H}_2^i \otimes \mathcal{H}_2^{i+2}\right]$ contains states of the form $\left\{ \underset{\in\mathcal{H}_2}{|\phi_j\rangle} \otimes \underset{\in\mathcal{H}_{0,1}}{\left|\psi_j^{J=0,1}\right\rangle} \right\}_{j=1,\ldots,4}$, where the four states $\left|\psi_j^{J=0,1}\right\rangle$ form a basis of $\mathcal{H}_{0,1}$ and $|\phi_j\rangle$ are some states in $\mathcal{H}_2$. Similarly, it also contains $\left\{ \underset{\in\mathcal{H}_{0,1}}{\left|\psi_j^{J=0,1}\right\rangle} \otimes \underset{\in\mathcal{H}_2}{|\phi_j\rangle} \right\}_{j=1,\ldots,4}$. By another application of K^i (respectively, K^{i+2}) acting only on $|\phi_j\rangle \in \mathcal{H}_2^i$ (respectively, $\mathcal{H}_2^{i+2}$), we generate both $\mathcal{H}_2^i \otimes \mathcal{H}_0^{i+2}$ and $\mathcal{H}_0^i \otimes \mathcal{H}_2^{i+2}$. This works because K^i contains any (Hermitian) operator on $\mathcal{H}_2$ such that $K^i\left[|\phi_j\rangle \otimes \left|\psi_j^{J=0,1}\right\rangle\right] = \mathcal{H}_2^i \otimes \left|\psi_j^{J=0,1}\right\rangle$ and likewise $K^{i+2}\left[\left|\psi_j^{J=0,1}\right\rangle \otimes |\phi_j\rangle\right] = \left|\psi_j^{J=0,1}\right\rangle \otimes \mathcal{H}_2^i$.

This mechanism works in general and allows us to generate any Hilbert-space summands with arbitrary number of $\mathcal{H}_{0,1}$ on arbitrary links by alternating application of the kernelizers on even and odd links. The only Hilbert-space summand not entirely accessible in this way is $\mathcal{H}_{0,1}^{\text{odd}} \equiv \bigotimes_{i=1,\,\text{odd}}^{N} \mathcal{H}_{0,1}^i$ and we conclude that $\mathcal{H}\backslash\mathcal{H}_{0,1}^{\text{odd}} \subset V$.

In order to connect all excited states in $\mathcal{H}_{0,1}^{\text{odd}}$ to $|v_0\rangle$, we now cover the whole chain by adjacent *even* links $(2,3), (3,4), \ldots, (N,1)$. First, note that $|v_0\rangle \in \mathcal{H}_2^{\text{even}}$. Thus we can repeat the above procedure and immediately find that $\mathcal{H}\backslash\mathcal{H}_{0,1}^{\text{even}} \subset V$. In order to show that V contains all states except $|\psi_{\text{AKLT}}\rangle$, we consider the orthogonal complement $V^\perp$. Note that $\left(\mathcal{H}\backslash\mathcal{H}_{0,1}^{\text{even}}\right) + \left(\mathcal{H}\backslash\mathcal{H}_{0,1}^{\text{even}}\right) \subseteq V$; therefore, $V^\perp \subseteq \left(\left(\mathcal{H}\backslash\mathcal{H}_{0,1}^{\text{even}}\right) + \left(\mathcal{H}\backslash\mathcal{H}_{0,1}^{\text{even}}\right)\right)^\perp = \left(\mathcal{H}\backslash\mathcal{H}_{0,1}^{\text{even}}\right)^\perp \cap \left(\mathcal{H}\backslash\mathcal{H}_{0,1}^{\text{even}}\right)^\perp = \mathcal{H}_{0,1}^{\text{odd}} \cap \mathcal{H}_{0,1}^{\text{even}}$. The only state not in V is simultaneously in the ground space of all even and all odd links. The only state in this set is the unique ground state $|\psi_{\text{AKLT}}\rangle$. This concludes the proof of controllability for even chain lengths.

For odd chain lengths, covering the whole chain by adjacent even and odd links leaves a single site uncovered, e.g., for 5 sites one would cover $(1,2), (3,4)$ or $(2,3)$ $(4,5)$. In other words, the chain essentially becomes a chain with open boundary conditions. We can still apply the above procedure but without the closing link $(N,1)$ there are now four states in $V^\perp$: the four degenerate AKLT ground states of a chain with open boundary conditions. To formalize this, $V^\perp \subseteq \mathcal{H}_{0,1}^{\text{odd}} \cap \mathcal{H}_{0,1}^{\text{even}}$ is not cut with $\mathcal{H}_{0,1}^N$ and therefore the states in $V^\perp$ are not constraint on $\mathcal{H}_{0,n}^N$, resulting in the four degenerate AKLT states. We can partition the four states in $V^\perp$ into $3+1$ states: one state without excitations on link N, corresponding to the unique AKLT ground state of a chain with PBCs; and the other three excited on link N and therefore subject to K^N, which allows us to connect them to V. This concludes the proof of controllability for odd chain lengths.

APPENDIX E: DIFFUSION WITH A SINK

We present a diffusive model of a relaxation problem in a 1D system with a pointlike sink (mimicking a measured link in the AKLT system). The motivation for such a description comes from the fact that elementary excitations of the AKLT model are weakly interacting local objects (solitons, "domain walls"; see Ref. [77]). These excitations are expected to diffuse on spatial scales larger than the mean free path determined by their interaction. The diffusive nature of their dynamics can also be inferred from the Wigner-Dyson character of the many-body level statistics (see Fig. 1 in Ref. [70]). Note that according to Ref. [70], there are separate species (sectors) of excitations (corresponding to different sets of quantum numbers) that interact within the sector but not with excitations from other sectors. Thus, the fluid of excitations splits into a set of mutually noninteracting fluids, as a result of the "partial integrability" of the AKLT model. In what follows, we consider a single fluid; all the spatial scales are assumed to be larger than the mean free path in this fluid of excitations—hence, we model the fluid with a diffusive equation.

1. Sink as a delta-function source term

Consider a 1D diffusion equation on a segment $[-L/2, L/2]$ with a delta-function sink term located at $x = 0$:

$$\frac{\partial}{\partial t} f(x,t) = D \frac{\partial^2}{\partial x^2} f(x,t) - A\,\delta(x) f(x,t), \tag{E1}$$

where A describes the strength of the pointlike sink that removes particles from the system and D is the diffusion constant. The sink strength is related to the absorption rate γ as $A = \ell\gamma$, where ℓ is the "ultraviolet" length scale of the problem.

We impose PBCs at $x = \pm L/2$. At time $t = 0$, a particle is located at $x = x_0$:

$$f(x,0) = \delta(x - x_0). \tag{E2}$$

At the position of the sink, the distribution function is continuous, $f(0-\delta, t) = f(0+\delta, t) = f(0,t)$, with infinitesimal $\delta \to 0$, while the derivative of the distribution jumps:

$$\left.\frac{\partial f}{\partial x}\right|_{x=0+\delta} - \left.\frac{\partial f}{\partial x}\right|_{x=0-\delta} = \frac{A}{D} f(0,t). \tag{E3}$$

Making use of the periodicity of the system, it is convenient to consider a segment $[0, L]$ instead of $[-L/2, L/2]$:

in this case, there is no need to impose an additional boundary condition at $\pm L/2$. We then have the boundary conditions relating the distribution function (and its derivative) only at $x = 0$ and $x = L$:

$$f(0,t) = f(L,t), \tag{E4}$$

$$\left.\frac{\partial f}{\partial x}\right|_{x=0} - \left.\frac{\partial f}{\partial x}\right|_{x=L} = \frac{A}{D} f(0,t). \tag{E5}$$

The general solution for the distribution function can be written in terms of symmetric (with respect to $x = L/2$) and antisymmetric parts:

$$f(x,t;x_0) = f_a(x,t;x_0) + f_s(x,t;x_0), \tag{E6}$$

$$f_a(x,t;x_0) = -f_a(L-x,t;x_0), \tag{E7}$$

$$f_s(x,t;x_0) = f_s(L-x,t;x_0). \tag{E8}$$

The antisymmetric part has zero at $x = 0$: otherwise, the derivatives at $x = 0$ and $x = L$ in Eq. (E5) would not match the boundary condition at the sink. This means that the antisymmetric part is not affected by the sink. The symmetric part has a finite value at $x = 0$ and L: otherwise, a finite difference of derivatives in Eq. (E5) is impossible.

The distribution function is represented in terms of a series of eigenmodes

$$e^{-Dtq^2}\sin(q(x-L/2)) \quad \text{and} \quad e^{-Dtq^2}\cos(q(x-L/2)),$$

which are solutions of the diffusion equation under the periodicity constraint. The antisymmetric part is independent of A,

$$f_a(x,t;x_0) = \frac{1}{L}\sum_{k=1}^{\infty} e^{-(\pi k/L)^2 Dt} \times \sin\left[\frac{\pi k}{L}\left(x_0 - \frac{L}{2}\right)\right]\sin\left[\frac{\pi k}{L}\left(x - \frac{L}{2}\right)\right], \tag{E9}$$

and corresponds to the solution of the 1D Schrödinger equation in a well with infinite walls at $x = 0$ and $x = L$ and a node at $x = L/2$. Replacing the sum over k with an integral in Eq. (E9) (which is, in fact, a dangerous procedure; see below), one obtains a natural result

$$f_a(x,t;x_0) \approx \frac{e^{-(x-x_0)^2/4Dt} - e^{-(L-x-x_0)^2/4Dt}}{2\sqrt{4\pi Dt}}, \tag{E10}$$

which describes the diffusive spreading of

$$f_a(x,0;x_0) = \frac{1}{2}\left[\delta(x-x_0) - \delta(x-L+x_0)\right].$$

Diffusion leads to a suppression of this channel with time due to the gradual homogenization of the distribution. The characteristic time scale is determined by the exponent for the slowest mode with $k = 1$. Since the antisymmetric part does not contribute to the particle number (or survival probability), we disregard f_a in what follows.

The symmetric part has the initial condition of the form

$$f_s(x,0;x_0) = \frac{1}{2}\left[\delta(x-x_0) + \delta(x-L+x_0)\right].$$

This distribution spreads according to

$$f_s(x,t;x_0) = \frac{1}{L}\sum_{n=1}^{\infty} e^{-q_n^2 Dt} \times \cos\left[q_n\left(x_0 - \frac{L}{2}\right)\right]\cos\left[q_n\left(x - \frac{L}{2}\right)\right]. \tag{E11}$$

The spectrum is determined by the (standard for quantum wells of finite depth) equation resulting from Eq. (E5):

$$Q_n \tan Q_n = \frac{AL}{4D}, \tag{E12}$$

where we have introduced a dimensionless wave vector

$$Q_n \equiv q_n L/2. \tag{E13}$$

We illustrate Eq. (E12) in Fig. 7. In view of the symmetry of f_s, we can consider only positive eigenvalues.

One should distinguish between the following two cases:

$$\text{(i)}\ AL/D \ll 1, \quad \text{(ii)}\ AL/D \gg 1. \tag{E14}$$

In case (i), the wave vector of the lowest eigenmode is special (see Fig. 7), as the left-hand side of Eq. (E12) is

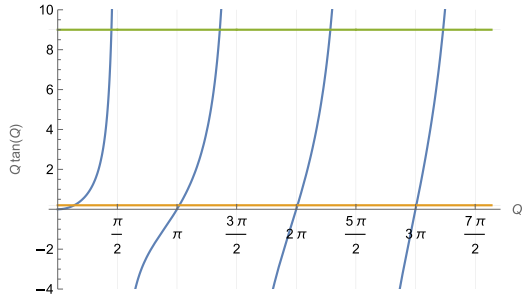

FIG. 7. The graphical representation of Eq. (E12). The spectrum is given by the values of Q for the intersections of the blue curve $Q\tan Q$ with the horizontal line that shows the right-hand side of Eq. (E12). The orange (green) line corresponds to $AL/4D \ll 1$ ($AL/4D \gg 1$).

quadratic in Q for $Q \ll 1$. This yields

$$Q_1^2 \simeq \frac{AL}{4D} \Rightarrow q_1 \simeq \sqrt{\frac{A}{DL}}. \tag{E15}$$

All the higher modes have the eigenvalues Q_n close to multiples of π, yielding

$$q_n \simeq \frac{2(n-1)\pi}{L} + \frac{A}{2\pi D(n-1)} \approx \frac{2(n-1)\pi}{L}, \quad n > 1. \tag{E16}$$

Since $q_1 \ll q_{n>1}$, the lowest mode decays much more slowly than other modes. As a result, for times $t \gg t_D$, where

$$t_D = L^2/D \tag{E17}$$

is the diffusion time of spreading over the system, the distribution is approximated by the lowest mode:

$$f_s(x,t;x_0) \approx \frac{1}{L}\exp\left(-\frac{A}{L}t\right)\cos\left[\sqrt{\frac{A}{DL}}\left(x_0 - \frac{L}{2}\right)\right] \times \cos\left[\sqrt{\frac{A}{DL}}\left(x - \frac{L}{2}\right)\right]. \tag{E18}$$

Note that the decay time t_A in this case is independent of D:

$$t_A = L/A. \tag{E19}$$

Integrating Eq. (E18) over x, we obtain the survival probability, which turns out to be essentially independent of x_0 ($L \ll \sqrt{Dt_A}$):

$$\begin{aligned} S(t) &\equiv \int_0^L dx f_s(x,t;x_0) \\ &\approx \frac{2\sqrt{Dt_A}}{L}\sin\left(\frac{L}{2\sqrt{Dt_A}}\right)\cos\frac{x_0 - L/2}{\sqrt{Dt_A}}\exp\left(-\frac{t}{t_A}\right) \\ &\approx \exp\left(-\frac{t}{t_A}\right). \end{aligned} \tag{E20}$$

Thus, in case (i), i.e., when the system is short or the absorption is weak, the "gap" scales as $1/L$.

In case (ii), the lowest eigenvalues Q_n are close to odd multiples of $\pi/2$ (see Fig. 7):

$$q_n \simeq (2n-1)\frac{\pi}{L} - (2n-1)\frac{\pi}{L}\frac{D}{AL}, \quad n \ll AL/D. \tag{E21}$$

For large values of n, the eigenvalues Q_n approach multiples of π, yielding

$$q_n \simeq 2n\frac{\pi}{L} + \frac{A}{DL\pi n}, \quad n \gg AL/D. \tag{E22}$$

For very long times, $t \gg t_D$, only the lowest mode with $n = 1$ can be retained:

$$f_s(x, t \gg t_D; x_0) \approx \frac{1}{L}\exp\left(-\frac{\pi^2}{L^2}Dt\right)\sin\frac{\pi x_0}{L}\sin\frac{\pi x}{L}. \tag{E23}$$

Note that the sink strength A does not enter this result, as we have neglected the subleading term in the spectrum in Eq. (E21). The survival probability is then given by

$$S(t \gg t_D, x_0) \approx \frac{2}{\pi}\sin\frac{\pi x_0}{L}\exp\left(-\frac{t}{t_D}\right). \tag{E24}$$

This corresponds to the "gap" that scales as $1/L^2$ (see Eq. (E17)).

The above results for the gap scaling are relevant for a finite-length system at the longest times, $t \to \infty$. In other words, they correspond to the following order of taking the "the thermodynamic limit":

$$\text{first } t \to \infty, \quad \text{then } L \to \infty. \tag{E25}$$

The opposite order of limits,

$$\text{first } L \to \infty, \quad \text{then } t \to \infty, \tag{E26}$$

corresponds to evolution in an infinite chain. A natural question in this case is whether the survival probability for a fixed x_0 tends to zero as $t \to \infty$ or the particle has a chance to escape absorption. For $A \to \infty$, the answer is clear: the problem reduces to the first-passage problem in 1D diffusion, where it is guaranteed that, within an infinite time interval, a random walker eventually visits $x = 0$, i.e., the survival probability indeed tends to zero. In our case, however, the absorption strength is finite. Related interesting questions can be asked about the fate of the random walker when the initial point itself scales with L, say, $x_0 = L/2$ or $x_0 \propto L^{1/2}$. In general, one can consider a distribution of initial points and this distribution can also evolve with the system size. Needless to say, taking the limit $L \to \infty$ first allows one to analyze the survival probability in a finite system at times shorter than the dwell time t_D.

The general expression for the survival probability reads

$$S(t,x_0) = 2\sum_{n=1}^{\infty} e^{-q_n^2 Dt}\cos\left[q_n\left(x_0 - \frac{L}{2}\right)\right]\frac{\sin(q_n L/2)}{q_n L}. \tag{E27}$$

Since we are interested here in the limit $L \to \infty$, we concentrate on case (ii), where $L \gg D/A$. Replacing, after

some massaging, the summation over n with the integration over q (see details in Appendix E 2), we obtain, for $L \to \infty$,

$$S(t,x_0) \simeq \int_0^{\sim A/D} \frac{dq}{\pi} e^{-q^2 Dt} \left[\frac{\sin(qx_0)}{q} + \frac{D}{2A} \cos(qx_0) \right]. \tag{E28}$$

We note that the upper limit of the integral is determined only up to a constant, but this constant is immaterial for the leading long-time asymptotics of $S(t)$, which read as follows:

$$S(t,x_0) \simeq \frac{2Ax_0 + D}{4A\sqrt{\pi Dt}} \operatorname{erf}\left(A\sqrt{\frac{t}{D}} \right) \overset{t\to\infty}{\approx} \frac{\sqrt{D}}{4A\sqrt{\pi t}}, \quad x_0 \ll D/A, \tag{E29}$$

and

$$S(t,x_0) \simeq \frac{1}{2} \operatorname{erf}\left(\frac{x_0}{\sqrt{4Dt}} \right) + \frac{\sqrt{D}}{4A\sqrt{\pi t}} \exp\left(-\frac{x_0^2}{4Dt} \right) \overset{t\to\infty}{\approx} \frac{x_0}{2\sqrt{\pi Dt}}, \quad x_0 \gg D/A, \tag{E30}$$

where

$$\operatorname{erf}(z) \simeq \begin{cases} \dfrac{2z}{\sqrt{\pi}}, & z \ll 1, \\ 1 - \dfrac{e^{-z^2}}{\sqrt{\pi}\, z}, & z \gg 1 \end{cases} \tag{E31}$$

is the error function.

We observe that, for a fixed value of x_0, the limit $L \to \infty$ can indeed be taken first: the remaining expression is finite and its time dependence is governed by the relation between x_0 and D/A. In any case, the long-time asymptotics of the survival probability in an infinite system is inversely proportional to the square root of time. Interestingly, for $x_0 \gg D/A$, the leading term is independent of the absorption strength A [see Eq. (E30)]. In finite systems, the obtained results for $S(t,x_0)$ are valid in the time window $t \ll t_D$; for longer times, the power-law suppression transforms into the exponential decay governed by the rate $1/t_D$ [see Eq. (E24)].

Thus, within this diffusive model, depending on the relation between the system size L and the characteristic lengths encoded by the parameters of the system, we can observe the following types of relaxation behavior:

(1) Short systems, $L \ll \ell$, where ℓ is the mean free path with respect to the interaction of elementary excitations: a "ballistic regime" with the relaxation rate determined by the measurement rate γ and the many-body level spacing as described in the main text.
(2) $\ell \ll L \ll D/A$, an intermediate diffusion regime: the exponential decay is determined by $t_A = L/A$, where $A = \ell\gamma$ and D is the diffusion constant (itself determined by ℓ).
(3) $L \gg D/A$: the time dependence of the survival probability is first given by $t^{-1/2}$ but at $t \gg t_D = L^2/D$ it becomes exponential, with the "gap" given by $1/t_D$. In the limit of an infinite system, an elementary excitation decays in the power-law (square-root) manner (implying zero gap for $L = \infty$, as it should be).

2. Evaluation of the sums in survival probabilities

In this section, we evaluate the sum in Eq. (E27) to derive the long-time asymptotics of the survival probability in an infinite system (the limit $L \to \infty$ is taken before sending $t \to \infty$). For $t \ll t_D$, when many eigenvalues contribute to the sum, it is natural to replace the summation over n in Eq. (E27) by integration over q. One should, however, exercise a certain caution when going from the sum to the integral over q. Indeed, we note that the factor $\sin(q_n L/2)$ in the sum in Eq. (E27) is exactly zero for the leading terms $q_n \approx 2n\pi/l$ in the spectrum for $n \gg AL/D$ given by Eq. (E22). This means that when neglecting the subleading terms in the spectrum, we should set the upper integration limit to A/D. For $q > A/D$, we should take into account the subleading terms in the spectrum,

$$\sin\frac{q_n L}{2} \simeq (-1)^n \frac{2A}{DL^2 q_n}, \quad n \gg \frac{AL}{D}.$$

For $n \gg AL/D$, we thus replace

$$\cos\left[q_n \left(x_0 - \frac{L}{2} \right) \right] \frac{\sin(q_n L/2)}{q_n L} \simeq \frac{A}{DL^2 q_n^2} \cos(q_n x_0)$$

in Eq. (E27). Similarly, using Eq. (E21) for $n \ll AL/D$, we can make another replacement in Eq. (E27) to take into account the discreteness of levels:

$$\cos\frac{q_n L}{2} \simeq (-1)^n \frac{D}{2A} q_n \quad \text{and} \quad \sin\frac{q_n L}{2} \simeq (-1)^{n+1},$$

which leads to

$$\cos\left[q_n \left(x_0 - \frac{L}{2} \right) \right] \frac{\sin(q_n L/2)}{q_n L} \simeq \frac{\sin(q_n x_0)}{q_n L} + \frac{D}{2AL} \left(1 - \frac{2x_0}{L} \right) \cos(q_n x_0).$$

As a result, we rewrite the sum in Eq. (E27) as

$$S(t,x_0) = 2\sum_{n=1}^{\sim AL/D} e^{-q_n^2 Dt}\left[\frac{\sin(q_n x_0)}{q_n L} + \frac{D}{2AL}\left(1-\frac{2x_0}{L}\right)\cos(q_n x_0)\right] + 2\sum_{\sim AL/D}^{\infty} e^{-q_n^2 Dt}\frac{A}{DL^2 q_n^2}\cos(q_n x_0). \tag{E32}$$

The value of n at which the sum in Eq. (E27) splits into two distinct sums in Eq. (E32) is not determined precisely; hence $n \sim AL/D$. This uncertainty, however, does not affect the long-time behavior of the survival probability. Now, it is safe to transform the sum into the integral, since no zeros appear for the leading terms in discrete q_n. After this transformation, for the contribution of $n > AL/D$ (second sum), we will have

$$\frac{1}{L^2}\sum_{AL/D}^{\infty}\ldots \mapsto \frac{1}{L}\int_{A/D}^{\infty}\frac{dq}{2\pi}\ldots,$$

which will vanish in the limit $L \to \infty$. Thus, we are left with the contribution of the first sum in Eq. (E32), i.e., terms with $n < AL/D$. Neglecting the term with $2x_0/L$, which also vanishes for $L \to \infty$ in the integral, we finally obtain Eq. (E28).

[1] J. F. Poyatos, J. I. Cirac, and P. Zoller, Quantum reservoir engineering with laser cooled trapped ions, Phys. Rev. Lett. **77**, 4728 (1996).

[2] S. Diehl, A. Micheli, A. Kantian, B. Kraus, H.-P. Büchler, and P. Zoller, Quantum states and phases in driven open quantum systems with cold atoms, Nat. Phys. **4**, 878 (2008).

[3] B. Kraus, H. P. Büchler, S. Diehl, A. Kantian, A. Micheli, and P. Zoller, Preparation of entangled states by quantum Markov processes, Phys. Rev. A **78**, 042307 (2008).

[4] F. Verstraete, M. M. Wolf, and J. Ignacio Cirac, Quantum computation and quantum-state engineering driven by dissipation, Nat. Phys. **5**, 633 (2009).

[5] S. Diehl, E. Rico, M. A. Baranov, and P. Zoller, Topology by dissipation in atomic quantum wires, Nat. Phys. **7**, 971 (2011).

[6] X. Mi, *et al.*, Stable quantum-correlated many-body states through engineered dissipation, Science **383**, 1332 (2024).

[7] T. Brown, E. Doucet, D. Ristè, G. Ribeill, K. Cicak, J. Aumentado, R. Simmonds, L. Govia, A. Kamal, and L. Ranzani, Trade off-free entanglement stabilization in a superconducting qutrit-qubit system, Nat. Commun. **13**, 3994 (2022).

[8] P. M. Harrington, E. J. Mueller, and K. W. Murch, Engineered dissipation for quantum information science, Nat. Rev. Phys. **4**, 660 (2022).

[9] H. M. Wiseman and G. J. Milburn, *Quantum Measurement and Control* (Cambridge University Press, Cambridge, 2009).

[10] S. Haroche and J. M. Raimond, *Exploring the Quantum: Atoms, Cavities, and Photons* (Oxford University Press, Oxford, 2006).

[11] S. Pielawa, G. Morigi, D. Vitali, and L. Davidovich, Generation of Einstein-Podolsky-Rosen-entangled radiation through an atomic reservoir, Phys. Rev. Lett. **98**, 240401 (2007).

[12] F. Ciccarello, S. Lorenzo, V. Giovannetti, and G. M. Palma, Quantum collision models: Open system dynamics from repeated interactions, Phys. Rep. **954**, 1 (2022).

[13] M. Raghunandan, F. Wolf, C. Ospelkaus, P. O. Schmidt, and H. Weimer, Initialization of quantum simulators by sympathetic cooling, Sci. Adv. **6**, eaaw9268 (2020).

[14] S. Polla, Y. Herasymenko, and T. E. O'Brien, Quantum digital cooling, Phys. Rev. A **104**, 012414 (2021).

[15] L. Marti, R. Mansuroglu, and M. J. Hartmann, Efficient quantum cooling algorithm for fermionic systems, arXiv:2403.14506.

[16] D. Burgarth and V. Giovannetti, Full control by locally induced relaxation, Phys. Rev. Lett. **99**, 100501 (2007).

[17] D. Burgarth and V. Giovannetti, Mediated homogenization, Phys. Rev. A **76**, 062307 (2007).

[18] P. O. Boykin, T. Mor, V. Roychowdhury, F. Vatan, and R. Vrijen, Algorithmic cooling and scalable NMR quantum computers, Proc. Natl. Acad. Sci. **99**, 3388 (2002).

[19] M. Metcalf, J. E. Moussa, W. A. de Jong, and M. Sarovar, Engineered thermalization and cooling of quantum many-body systems, Phys. Rev. Res. **2**, 023214 (2020).

[20] M. P. Zaletel, A. Kaufman, D. M. Stamper-Kurn, and N. Y. Yao, Preparation of low entropy correlated many-body states via conformal cooling quenches, Phys. Rev. Lett. **126**, 103401 (2021).

[21] K. Rojan, D. M. Reich, I. Dotsenko, J.-M. Raimond, C. P. Koch, and G. Morigi, Arbitrary-quantum-state preparation of a harmonic oscillator via optimal control, Phys. Rev. A **90**, 023824 (2014).

[22] S. Roy, J. T. Chalker, I. V. Gornyi, and Y. Gefen, Measurement-induced steering of quantum systems, Phys. Rev. Res. **2**, 033347 (2020).

[23] P. Kumar, K. Snizhko, and Y. Gefen, Engineering two-qubit mixed states with weak measurements, Phys. Rev. Res. **2**, 042014 (2020).

[24] D. Perez-Garcia, F. Verstraete, M. M. Wolf, and J. I. Cirac, PEPS as unique ground states of local Hamiltonians, Quantum Inf. Comput. **8**, 650 (2008).

[25] P. D. Johnson, F. Ticozzi, and L. Viola, General fixed points of quasi-local frustration-free quantum semigroups: From invariance to stabilization, Quantum Inf. Comput. **16**, 657 (2016).

[26] F. Ticozzi and L. Viola, Steady-state entanglement by engineered quasi-local Markovian dissipation:

Hamiltonian-assisted and conditional stabilization, Quantum Inf. Comput. **14**, 265 (2014).
[27] M. P. Fisher, V. Khemani, A. Nahum, and S. Vijay, Random quantum circuits, Annu. Rev. Condens. Matter Phys. **14**, 335 (2023).
[28] C. Noel, P. Niroula, D. Zhu, A. Risinger, L. Egan, D. Biswas, M. Cetina, A. V. Gorshkov, M. J. Gullans, D. A. Huse, and C. Monroe, Measurement-induced quantum phases realized in a trapped-ion quantum computer, Nat. Phys. **18**, 760 (2022).
[29] J. M. Koh, S.-N. Sun, M. Motta, and A. J. Minnich, Measurement-induced entanglement phase transition on a superconducting quantum processor with mid-circuit readout, Nat. Phys. **19**, 1314 (2023).
[30] J. C. Hoke, *et al.*, Google Quantum AI and Collaborators, Measurement-induced entanglement and teleportation on a noisy quantum processor, Nature **622**, 481 (2023).
[31] J.-J. Feng, B. Wu, and F. Wilczek, Quantum computing by coherent cooling, Phys. Rev. A **105**, 052601 (2022).
[32] A. Matthies, M. Rudner, A. Rosch, and E. Berg, Programmable adiabatic demagnetization for systems with trivial and topological excitations, arXiv:2210.17256.
[33] G. Kishony, M. S. Rudner, A. Rosch, and E. Berg, Gauged cooling of topological excitations and emergent fermions on quantum simulators, arXiv:2310.16082.
[34] V. Maurya, H. Zhang, D. Kowsari, A. Kuo, D. M. Hartsell, C. Miyamoto, J. Liu, S. Shanto, E. Vlachos, A. Zarassi, K. W. Murch, and E. M. Levenson-Falk, On-demand driven dissipation for cavity reset and cooling, PRX Quantum **5**, 020321 (2024).
[35] T. Fogarty, H. Landa, C. Cormick, and G. Morigi, Optomechanical many-body cooling to the ground state using frustration, Phys. Rev. A **94**, 023844 (2016).
[36] A. Biella and M. Schiró, Many-body quantum Zeno effect and measurement-induced subradiance transition, Quantum **5**, 528 (2021).
[37] T. Albash and D. A. Lidar, Adiabatic quantum computation, Rev. Mod. Phys. **90**, 015002 (2018).
[38] R. Menu, J. Langbehn, C. P. Koch, and G. Morigi, Reservoir-engineering shortcuts to adiabaticity, Phys. Rev. Res. **4**, 033005 (2022).
[39] A. Paviglianiti, X. Turkeshi, M. Schirò, and A. Silva, Enhanced entanglement in the measurement-altered quantum Ising chain, arXiv:2310.02686.
[40] Y. Herasymenko, I. Gornyi, and Y. Gefen, Measurement-driven navigation in many-body Hilbert space: Active-decision steering, PRX Quantum **4**, 020347 (2023).
[41] I. Affleck, T. Kennedy, E. H. Lieb, and H. Tasaki, Rigorous results on valence-bond ground states in antiferromagnets, Phys. Rev. Lett. **59**, 799 (1987).
[42] I. Affleck, T. Kennedy, E. H. Lieb, and H. Tasaki, Valence bond ground states in isotropic quantum antiferromagnets, Commun. Math. Phys. **115**, 477 (1988).
[43] B. Murta, P. M. Q. Cruz, and J. Fernández-Rossier, Preparing valence-bond-solid states on noisy intermediate-scale quantum computers, Phys. Rev. Res. **5**, 013190 (2023).
[44] K. C. Smith, E. Crane, N. Wiebe, and S. Girvin, Deterministic constant-depth preparation of the AKLT state on a quantum processor using fusion measurements, PRX Quantum **4**, 020315 (2023).
[45] T. Chen, R. Shen, C. H. Lee, and B. Yang, High-fidelity realization of the AKLT state on a NISQ-era quantum processor, SciPost Phys. **15**, 170 (2023).
[46] T. Chen and T. Byrnes, Efficient preparation of the AKLT state with measurement-based imaginary time evolution, arXiv:2310.06031.
[47] D. A. Puente, F. Motzoi, T. Calarco, G. Morigi, and M. Rizzi, Quantum state preparation via engineered ancilla resetting, Quantum **8**, 1299 (2024).
[48] A. Sriram, T. Rakovszky, V. Khemani, and M. Ippoliti, Topology, criticality, and dynamically generated qubits in a stochastic measurement-only Kitaev model, Phys. Rev. B **108**, 094304 (2023).
[49] A. Lavasani, Z.-X. Luo, and S. Vijay, Monitored quantum dynamics and the Kitaev spin liquid, Phys. Rev. B **108**, 115135 (2023).
[50] S. Morales, Y. Gefen, I. Gornyi, A. Zazunov, and R. Egger, Engineering unsteerable quantum states with active feedback, Phys. Rev. Res. **6**, 013244 (2024).
[51] C. Sayrin, I. Dotsenko, X. Zhou, B. Peaudecerf, T. Rybarczyk, S. Gleyzes, P. Rouchon, M. Mirrahimi, H. Amini, M. Brune, J.-M. Raimond, and S. Haroche, Real-time quantum feedback prepares and stabilizes photon number states, Nature **477**, 73 (2011).
[52] D. Volya and P. Mishra, Fl state preparation on quantum computers via quantum steering, IEEE Trans. Quantum Eng. **5**, 1 (2024).
[53] C. K. Majumdar and D. K. Ghosh, On next-nearest-neighbor interaction in linear chain. I, J. Math. Phys. **10**, 1388 (2003).
[54] H.-P. Breuer and F. Petruccione, *The Theory of Open Quantum Systems* (Oxford University Press, Oxford, 2007).
[55] A. Rivas and S. F. Huelga, *Open Quantum Systems* (Springer-Verlag, Berlin, 2011).
[56] We assume here that $\mathcal{L}$ has no purely imaginary eigenvalues [58].
[57] D. Basilewitsch, C. P. Koch, and D. M. Reich, Quantum optimal control for mixed state squeezing in cavity optomechanics, Adv. Quantum Technol. **2**, 1800110 (2019).
[58] H. Yoshida, Uniqueness of steady states of Gorini-Kossakowski-Sudarshan-Lindblad equations: A simple proof, Phys. Rev. A **109**, 022218 (2024).
[59] V. V. Albert, Asymptotics of quantum channels: Conserved quantities, an adiabatic limit, and matrix product states, Quantum **3**, 151 (2019).
[60] F. Pollmann, E. Berg, A. M. Turner, and M. Oshikawa, Symmetry protection of topological phases in one-dimensional quantum spin systems, Phys. Rev. B **85**, 075125 (2012).
[61] F. Verstraete and J. I. Cirac, Valence-bond states for quantum computation, Phys. Rev. A **70**, 060302 (2004).
[62] Y. Wang, K. Snizhko, A. Romito, Y. Gefen, and K. Murch, Dissipative preparation and stabilization of many-body quantum states in a superconducting qutrit array, Phys. Rev. A **108**, 013712 (2023).
[63] F. Ticozzi and L. Viola, Stabilizing entangled states with quasi-local quantum dynamical semigroups, Proc. Trans. R. Soc. A: Math. Phys. Eng. Sci. **370**, 5259 (2012).
[64] J. Dalibard, Y. Castin, and K. Mølmer, Wave-function approach to dissipative processes in quantum optics, Phys. Rev. Lett. **68**, 580 (1992).

[65] The bootstrap resampling method [78] is useful to estimate quantities from a random distribution with low sample size. It also provides a simple way to assign confidence intervals and therefore standard deviations. The method works by repeatedly (here, 500 times) randomly resampling the data with replacement. Each of the resamples is used to estimate the quantities of interest and the final mean and variance are given by the resulting statistics.

[66] To be precise, nondilute cooling toward a GHZstate requires conditional stabilization, i.e., active steering [26]. Passive steering is possible when targeting a GHZ state only approximately [79].

[67] G. Morigi, J. Eschner, C. Cormick, Y. Lin, D. Leibfried, and D. J. Wineland, Dissipative quantum control of a spin chain, Phys. Rev. Lett. **115**, 200502 (2015).

[68] D. D'Alessandro, *Introduction to Quantum Control and Dynamics* (Chapman and Hall/CRC, New York, 2007), 1st ed.

[69] S. Roy, C. Otto, R. Menu, and G. Morigi, Rise and fall of entanglement between two qubits in a non-Markovian bath, Phys. Rev. A **108**, 032205 (2023).

[70] S. Moudgalya, S. Rachel, B. A. Bernevig, and N. Regnault, Exact excited states of nonintegrable models, Phys. Rev. B **98**, 235155 (2018).

[71] N. Defenu, T. Donner, T. Macrì, G. Pagano, S. Ruffo, and A. Trombettoni, Long-range interacting quantum systems, Rev. Mod. Phys. **95**, 035002 (2023).

[72] M. C. Tran, C.-F. Chen, A. Ehrenberg, A. Y. Guo, A. Deshpande, Y. Hong, Z.-X. Gong, A. V. Gorshkov, and A. Lucas, Hierarchy of linear light cones with long-range interactions, Phys. Rev. X **10**, 031009 (2020).

[73] E. Medina-Guerra, P. Kumar, I. V. Gornyi, and Y. Gefen, Quantum state engineering by steering in the presence of errors, Phys. Rev. Res. **6**, 023159 (2024).

[74] M. Cattaneo, G. De Chiara, S. Maniscalco, R. Zambrini, and G. L. Giorgi, Collision models can efficiently simulate any multipartite Markovian quantum dynamics, Phys. Rev. Lett. **126**, 130403 (2021).

[75] Y. Zhang and T. Barthel, Criteria for Davies irreducibility of Markovian quantum dynamics, J. Phys. A: Mathematical and Theoretical **57**, 115301 (2024).

[76] https://www.hqi.fr

[77] U. Neugebauer and H.-J. Mikeska, Domain wall theory of elementary excitations in anisotropic antiferromagnetic $S = 1$ chains, Z. Phys. B Condens. Matter **99**, 151 (1995).

[78] B. Efron, Bootstrap methods: Another look at the jackknife, Ann. Stat. **7**, 1 (1979).

[79] V. Martin and A. Sarlette, Stabilization of approximate GHZ state with quasi-local couplings, arXiv:2306.05070.